MODELING THE JAW MECHANICS OF *DIMETRODON* (SYNAPSIDA: SPHENACODONTIDAE)

By Adam Jeremy Snyder

A Thesis submitted to the Faculty of Graduate Studies of

The University of Manitoba

in partial fulfilment of the requirements of the degree of

MASTER OF SCIENCE

Department of Earth Sciences

Clayton. H Riddell Faculty of Environment, Earth, and Resources

University of Manitoba

Winnipeg

This work as printed and the individual chapters within is the sole authorship of

Adam J. Snyder.

Abstract

In this work, I investigate the biomechanics of a 295-million-year-old proto-mammal, *Dimetrodon,* using a series of models and experiments to recreate their jaw as accurately as possible. Using a combination of 2D images and computed tomography scans, virtual fossils were created in 3D. This project is the first use of finite element analysis and multibody dynamics analysis in the genus. For the first time, dental microanatomy including denticles and plicidentine was modelled in 3D with individual material properties. Three separate muscle topologies of *Dimetrodon* were sculpted for the first time in 3D to determine individual muscle performance and a maximum combined effective bite adduction force of 4000N.

Different tooth morphologies influenced the biomechanical performance of *Dimetrodon*'s bite. Both the incisiform and caniniform teeth were able to function effectively at maximum bite force; however, the post-caniniform teeth were unable to dissipate stress at these levels. Enamel denticles created complex patterns of localized stress across the enamel-dentine junction into the core of the crown. Elongation of the tooth roots increased the ability of the alveolar bone to cushion kinetic energy before being transmitted to the surrounding jawbone.

Examining the stress and strain distribution patterns through the skull of *Dimetrodon* necessitated revisiting proposed topologies of the animal's adductor musculature. The most recent reconstruction, the reptilian style of muscle attachment, is the most efficient arrangement of the muscles. The rhynchocephalian style had the highest muscle volume and produced a larger bite force estimate from the dry skull

method. Predictive models based on physiological cross-sectional muscle areas are cautioned against. This model returned a bite force similar to extant hypercarnivores, and combined with little fossil evidence of bone comminution, suggests *Dimetrodon* was not limited by prey size and could consume the flesh of large-bodied animals.

Acknowledgements

I wish to thank my advisor Kirstin Brink for her patience and support throughout the entire project. Eric Snively encouraged and was a valuable resource as I began my journey into fossil biomechanics. Lastly from my committee, Julia Gamble offered critical thinking challenges in the application of my work to broader biological contexts. Thank you to Masateru Shibata for assistance with and providing scanned fossil material. As well this project would be significantly handicapped without my lab mates at the University of Manitoba who ensured a remote connection through COVID and snowstorms. Finally, I would also like to thank my fellow graduate students in the Department of Earth Sciences (formerly Geological Sciences) who fostered a welcoming and incredibly supportive environment, whether on or offline.

This research was funded through a Research Manitoba Studentship, a travel grant from the Paleontological Society and an NSERC Discovery Grant awarded to Dr. Kirstin Brink.

Dedication

This project is dedicated to my family: Kim, Jeremy, Stuart, Ann, Henry, Dianne, and sister Kristine. Finally, to my mentors who framed interesting problems as fun challenges to solve.

Table of Contents

Contents

List of Tables

List of Figures

Chapter 1: Introduction

The Permian was one of the most remarkable periods in the history of life. The collation of the supercontinent Pangea influenced climate regionally and globally, resulting in massive ecosystem upheaval and the development of new niches. At the end of the Carboniferous, vertebrates reached a significant milestone in the development of the amniotic egg. This permitted full terrestriality and permanent colonization of these new ecosystems by vertebrates (Olson 1966; Sues and Reisz, 1998; Sahney et al., 2010; Brocklehurst et al., 2013). One early group to adapt to this new ecosystem was the sphenacodontids, a basal clade of non-mammalian synapsids. Although only representing a fraction of the diversity in this novel terrestrial ecosystem, the group saw success and rapid diversification, including the rise of the clade's most renowned member, *Dimetrodon* (Romer and Price 1940). Known from 14 distinct species across North America and Europe, *Dimetrodon* is typically recognized for neural spines that collectively formed an expansive sail (Huttenlocker et al., 2010). This adaptation is alien when compared to modern vertebrates but was prevalent across numerous taxa in the Early Permian (Mann and Reisz, 2020). While some nutrient cycling would continue to be obtained from nearby aquatic environments throughout the Early Permian, the terrestrial space finally supported a diversity of herbivorous and carnivorous vertebrates and would resemble the makeup of modern-day terrestrial ecosystems by the mid to late Permian following the extinction of *Dimetrodon* (Olson, 1966). *Dimetrodon* fossil material is often found alongside aquatic and amphibious taxa such as the shark *Xenacanthus* (Parrish, 1978) and the temnospondyl amphibian *Zatrachys* (Romer and Price, 1940; Bakker et al., 2015), but also with large-bodied herbivores (Sander, 1989). Therefore, it is not known if

Dimetrodon was capable of consuming large-bodied prey or exclusively fed on smaller, primarily aquatic taxa (Bakker, 1982). Potentially, their prey preferences changed throughout the evolution of Early Permian ecosystems. The biomechanical capabilities of *Dimetrodon* have not yet been assessed but may have permitted them to hunt herbivores rivalling or exceeding their own size (Moreno et al., 2008). The gradual acquisition of these feeding adaptations within *Dimetrodon* provides an interesting case study to examine the community-wide transition of vertebrates from aquatic-dominated ecosystems to dedicated terrestrial communities through a top-down ecological lens (Beschta and Ripple, 2009). Considering that *Dimetrodon* was at the top of the food chain, prey populations would have sequentially increased or decreased from predation levels as one descended trophically. *Dimetrodon*'s role in establishing modern-type terrestrial ecosystems is still not fully understood.

The Greek name *Dimetrodon* means 'two-measure teeth', an adaptation extrapolated from major differences between teeth anchored on the premaxilla and maxilla. Heterodonty would become widely adopted among derived synapsids but was rare this early in amniote evolution (Huttenlocker et al., 2021). Two to four broadened, spike-like incisiform teeth sit at the front of the jaw in the premaxilla. In some specimens, small teeth of this same morphology are present anterior to a prominent diastema containing the premaxilla's suture with the maxilla. In all species, the largest tooth is anchored immediately posterior to the diastema, creating a near fang-like dentition. This prominent tooth is the largest in the jaw and more caniniform in shape compared to those on the premaxilla, becoming more exaggerated in size and shape in derived members.

Progressively along the tooth row, caniniform teeth shrink along the cheek to become the smallest members of the primary dentition. While heterodonty allows for a more sophisticated diet through varied oral processing, its origin is difficult to assess in early synapsids. Amid major changes to tooth morphology and dental patterning is the acquisition of the pre-canine step and diastema shared between sphenacodontians (Spindler 2020). The proximity of these structures and their direct influence on feeding behaviours presents multiple questions: How did *Dimetrodon* make use of the different teeth in its jaw? Does heterodonty indicate ecological specialization or increased capabilities supporting a generalist diet? How does heterodonty influence *Dimetrodon* skull biomechanical performance?

Hypothesis #1: If the caniniform teeth transfer less stress onto the skull than the incisiform teeth, then *Dimetrodon*'s skull is preferentially mitigating kinetic energy surrounding this tooth position. Principles of biomechanical efficacy combined with inferences from extant tetrapods can inform feeding behaviours relating to heterodont dentitions in *Dimetrodon*.

Dimetrodon's ecological success is supported by multiple species overlapping temporally and spatially with high abundance relative to other Early Permian taxonomic groups (Berman et al., 2001). Between species, several functional differences and trends appear in the fossil record. Broadly, the group increased in size from the earliest species, *D. teutonis* and *D. milleri,* at an estimated length of one to two meters, to the latest member, *D. angelensis* reaching over four times that length (Romer, 1936; Romer and Price, 1940; Olson 1962; Berman et al., 2004; Brocklehurst and Brink, 2017). Beyond size,

variation exists in the vertebral spines that construct *Dimetrodon*'s iconic sail (Huttenlocker et al., 2010). Few changes occur in the cranial skeleton; the precanine step increases in height as does the coronoid process on the mandible (Romer and Price, 1940). In terms of tooth morphology, the earliest species exhibit plicidentine, an ancestral adaptation wherein the tooth roots have inward collapsing folds (Brink et al., 2014). While still recurved, the tooth crowns are smooth-edged or have subtle enamel serrations, contrasting with geologically younger species, where true ziphodonty (denticles formed by enamel and dentine) developed (Brink and Reisz, 2014). The younger species also have teeth with non-folded, deep tooth roots matching the length of their bladelike crowns (Brink et al., 2014). Undeniably the most derived members of *Dimetrodon* fit the dental suite of hyper-carnivorous traits better than any other member of the Early Permian (Abler, 1992). Adaptations to the teeth are often associated with food processing, in tandem with other skeletal elements such as the mandibular and palatal series. The biomechanical implications of this transitioning morphology have not been examined in the context of a single taxon before and may provide insight into any biomechanical differences between different species of *Dimetrodon.*

The different tooth morphologies appear later in the fossil record in various lineages of specialized taxa. Ziphodont teeth are present in theropod dinosaurs, therapsid synapsids, and modern varanid lizards (Brink et al., 2015, Abler 1992, Whitney et al., 2020). Ziphodont teeth excel in slicing through soft tissue (Abler 1992). This anatomy is noticeably different when compared to presumed fish-eating animals such as *Dimetrodon's* synapsid contemporaries, such as *Secodontosaurus* and *Ophiacodon,* and

crocodilians that comparatively excel at puncture and hold morphologies (Reisz et al., 1992). Differences in biomechanical efficiency between these two separate morphologies could indicate the primary diet of *Dimetrodon*, whether their teeth needed to process large-bodied prey items such as the terrestrial synapsid herbivore *Edaphosaurus* or hold slippery prey like the shark *Xenacanthus*

Hypothesis #2: If the tooth microstructure becomes more biomechanically efficient through evolutionary time, then *Dimetrodon* is adapting for greater masticatory loads, indicating a changing diet.

Dimetrodon dental biomechanics will be primarily investigated in my first chapter, and the relationship between heterodonty and its effects on the complete skull of *Dimetrodon* in the second chapter. Despite its complexity, *Dimetrodon* conserves the shape of skull elements between species (Case, 1907; Romer and Price, 1940). This presents a unique opportunity to examine functional variations intrinsically tied with feeding strategy and dietary development. These changes can be viewed as trends across geologic time but also complexities within their ecological communities; the red shale of the Arroyo formation in Texas hosts at least four co-occurring species (Romer and Price, 1940; Brink et al., 2015). It is currently uncertain how these differences in dentition and overall size influence community interactions and the overall function of the feeding apparatus.

As *Dimetrodon* is situated at a critical point in amniote phylogeny, muscle reconstructions have been based on shifting bias between mammalian- versus reptilian-style anatomy and lever systems (Watson, 1948; Fox, 1964; Demar and Barghusen, 1972).

The currently accepted model is a combination of the two, whereby *Dimetrodon* maintains the distribution and differentiation of reptilian jaw musculature but from a stage where the mammalian condition is recognizable and would derive (Barghusen, 1973). Possible calculations from these reconstructions were limited in their application, being able to impart a generalized force onto a simplified beam model (Thomason, 1991). Still, they could not simultaneously determine the functional output on the sharpest edges of socketed teeth. Despite limitations, adaptations to the coronoid step of *Dimetrodon* along with other non-mammalian synapsids are posited to have maximized torque and thereby power while adding muscle flexibility to resist variable directions of large prey item loading (Barghusen, 1973). The evolution of computerized methods can be used to empirically determine the validity of our older models and either ratify our confidence in them or inspire alternatives. One way to evaluate this is through the testing of paradigms in biologically supported similar reconstructions (Rudwick 1964). This methodology postulates that if our model is the most biomechanically efficient and is anatomically sound, then it is a robust basis for inference and further refinement. Based on these models, what is the maximum bite force of *Dimetrodon*?

In chapter three I will investigate the following hypotheses:

Hypothesis #3: If the reptilian muscle reconstruction more efficiently transmits force to the teeth on the lower mandible than other proposed reconstructions (rhynchocephalian and mammal), then that topology is supported biomechanically.

Hypothesis #4: If *Dimetrodon* had a bite force comparable to extant hypercarnivores, then it would not be biomechanically limited from processing large-bodied prey such as *Edaphosaurus*.

Biomechanical studies rely on the principle that phenotypic adaptations can be driven by energy efficiency. Skulls adapt from numerous sources of conflicting evolutionary pressure: minimizing skull weight to reduce neck muscle strain; providing sufficient surface area for key muscle attachment; maximizing the transmission of force through the teeth; and minimizing the self-inflicted stress from a bite are just a few examples (Preuschoft and Witzel, 2002). Fossil biomechanics paired with observational methods can examine traces on the bones of prey taxa that are attributed to a scavenger or predator's bites; this is reverse engineered to determine the force of the bite that imparted the wound (Erickson and Olson, 1996). Without these trace scars to work from, we must conduct our own experiments to determine functionality.

Digital Modelling Techniques

Experimental simulations have been developed to infer the biological constraints of organisms, with these maximum values being compared between taxa. The basis of most cranial studies can be traced to the beam model for estimating complex skull mechanics (Thomason, 1991). This study examined the bending stress (σ) of the skull by finding the forces exerted by the muscles and their bending moments and structural counteraction from the skull through areas, second-moment areas, and section moduli. The beam theory method with muscle values from the Dry Skull Method (DSM) tended to

underestimate the skull's forces compared to in-vivo results; however, this methodology has been tuned by biomechanically inclined paleontologists for decades.

Bone architecture is constructed in different ways throughout the body to best support non-rigid tissues, anchor muscles, and resist environmental forces. When subjected to a compressive force, a ductile reaction will absorb most but not all kinetic energy (Ehrlich and Lanyon, 2002; Dutel et al., 2021). The location of the highest variant concentrations may reach a maximum limit in which the forces are too high, causing a permanent deformation (yield strength) or complete break (absolute strength). This threshold is often used in biological studies as an animal is unlikely to be capable of breaking its own jaw through mandibular adduction, serving as the comparable limit between taxa. This variable in an isotropic environment is primarily influenced by the shape of the element, allowing for direct comparison between elements or a series, such as a skull, based upon the maximum distortion before irreversible failure. The von Mises stress (calibrated to material breaking point) is the critical variable for the present study to compare the stress of each *Dimetrodon* jaw. Derived from Hooke's law, this variable equates deviatoric stress with strain to give an indication of proximity to material failure in bone (Bourgoyne et al., 1986).

One modelling technique, Finite Element Analysis (FEA), was initially developed for mechanical engineering and typically applied to problems relating to the breaking points of structures or industrial objects (Edelsbrunner and Mucke, 1994). This technique represents objects as a network of interconnected polygons; their shape, size, and material properties are modified to best represent the testing scenario. It can be

performed both in two-dimensional work from single images and three-dimensions with a full volume afforded by computed tomography (CT). An appropriate balance of the number of shapes must be reached as too few will not mathematically represent the shape, and too many will waste computer processing power and time. These methods proved successful in their industrial applications and were integrated into modern biological and dental modelling applications (Sellers and Crompton, 2004; Ross and Metzger, 2004). The appeal of FEA in the paleontological sphere stems from its facility for non-destructive experimentation, a previous challenge when working with fossil data (Bright, 2014). To simulate the biomechanical function of an extinct organism, a representative geometry is created from the CT image derived from a specimen. Force applied at a point, or an area will then propagate stress and strain in a pattern unique to a skull or other structure.

Another methodology, Multi-body Dynamic Analysis (MDA), can bridge the gap between muscle-driven movements and bone stress. MDA allows the addition of simulated muscles to work cooperatively or antagonistically on the imported skeletal model (Dutel et al., 2021). The muscle fibres are represented as individual hydraulic units with strengths proportional to their size on the skull. These muscles are sequentially or unanimously activated to work on the bony elements to shut the gape or crush a food item. Through repeated simulations, the program can optimize the muscle activation patterns and allow for time correlation of the results.

Dimetrodon is an emblematic member of not only the Permian but the terrestrial Paleozoic. These animals represented the apex of terrestrial food webs and were the first

top predator to occupy this role. This project is the opportunity to examine this critical taxon's rapid success through biomechanical analysis of morphologically significant evolutionary changes. By drawing comparisons with force and stress patterns in extant taxa, we can interpret the behaviour and role of *Dimetrodon* in non-analogue Permian ecosystems. Adaptations in the teeth can inform inferences of evolutionary trajectories and environmental pressures that this group was subjected to during the establishment of modern terrestrial ecosystems that include the first large-bodied obligate herbivores. A focused examination of *Dimetrodon* as a high-level consumer provides a top-down ecological perspective into the Permian community, informing future studies focused not only on *Dimetrodon* but the other fossil members with which it shares a relationship.

Chapter 2: TOOTH BIOMECHANICS USING TWO- AND THREE-DIMENSIONAL FINITE ELEMENT ANALYSIS IN THE NON-MAMMALIAN SYNAPSID *DIMETRODON* INDICATES A SHIFT TO LARGE-BODIED PREY

Formatted for the Journal of the Royal Society Interface

https://royalsociety.org/journals/authors/author-guidelines/?_ga=2.22929659.1922168534.1654015609-541328327.1625675953

Abstract

Major changes in tooth morphology can be tracked within the evolutionary history of the Early Permian mammal precursor, *Dimetrodon* (295-270 MA). Through the evolution of the genus, teeth changed from the ancestral condition of folded roots (plicidentine) and crowns with smooth cutting edges (carinae) towards a ziphodont crown morphology with denticulate carinae and elongate roots typical of other extinct apex predators. Biomechanical investigation of this evolutionary change in *Dimetrodon* serves as a key opportunity to test if changes in tooth morphology correspond to changes in function and interpretations on feeding style. We created virtual models of individual teeth from photographs and computed tomography (CT) scans to

investigate the functional differences between these morphological conditions through a combination of 2D and 3D Finite Element Analyses (FEA). Material properties based on extant values of enamel, dentine, and bone were imported on models loaded with point forces directed at the tooth tips. Results show that in the crowns, denticles lessen the energy that reaches the core of the tooth. Providing an overall buffering effect, the denticles convey energy non-homogenously, funneling stress and strain to the thinnest enamel layers between the denticles. In the roots, increased surface area resulted in lower stress values in the tooth root. Similar areas in a short, folded root did not significantly alter energy transmitted to the cortical bone when compared to elongated, smooth roots. Plicidentine roots localized stress to fold crests. FEA results support the hypothesis that denticles and elongated, non-folded roots were all adaptations that would assist *Dimetrodon* in the oral processing of larger prey items.

Introduction

Tissues are among the most fundamental and important organizational units in biological systems. Combined, they constitute organ systems and specialized anatomical complexes that work towards a series of specific functions. The feeding apparatus, and the tissues therein, has primarily adapted in most vertebrates for the acquisition and oral processing of food. *Dimetrodon,* a non-therapsid synapsid (mammalian lineage vertebrate) from the Early Permian (295-270MA) is named after its heterodont dentition, a key feature used to support its position as an apex predator. Ziphodont teeth developed first among amniotes (terrestrial reproducing) in *Dimetrodon,* which is a tooth morphology recognizable from a recurved, knife-like crown shape and serrated edges to assist in soft-flesh slicing (1,2). During the 20-million-year evolutionary history of *Dimetrodon*, the morphology of the cutting edges (carinae) changed from being smooth in the oldest species (*D. milleri* and *D. teutonis*) to bearing irregular, dentine cored

and enamel-capped serrations (denticles) in the most derived species (1). Serrations evolved many times in fossil groups after *Dimetrodon* albeit in slightly different constructions that likely influence their biomechanical performance (2-4). *Dimetrodon* serrations in derived species are true denticles with irregular spacing and sizes relative to their neighbours (3). In some ziphodont species, such as theropod dinosaurs and therapsid synapsids, an interdental fold composed of globular mantle dentine sits just below a narrow channel that extends through the enamel between each denticle (3,4). The presence of an interdental fold likely helps to strengthen the serrations and to help create regularity in size and spacing along the carinae (3). While the interdental fold develops independently first in gorgonopsian therapsids and then also independently appears in theropod dinosaurs; these elements are completely absent in the denticles of *Dimetrodon* (1, 3).

Concurrent with crown modifications, the root changes from being short relative to the crown with folded roots in cross section (plicidentine) to lengthened, straight roots equal in size to the crown (3). Folded tooth roots increase the surface area of attachment, assisting adhesion to the jaw structure in a restricted root space (5,6). This was critical for crown amniotes with flattened skulls that limited, the dorso-ventral space for tooth roots. By the time of derived sphenacodontians such as *Dimetrodon*, the skull shape had increased the height of the maxilla to accommodate a lengthened tooth root. The most derived members of *Dimetrodon, including D. borealis and D. grandis* have long roots extending into the maxilla with no plicidentine (Fig 1) (7).

Amniote (terrestrial reproducing) contemporaries of *Dimetrodon* such as *Cotylorhynchus*, *Edaphosaurus* and *Diadectes* achieved large body sizes on a primarily herbivorous diet (8,9). Terrestrial herbivory had never been present in vertebrates previously, constraining trophic diversity in the Late Carboniferous (10). An expanding ecology supported larger-bodied predators, allowing *Dimetrodon* to be among the first terrestrial amniote carnivores in Earth's history. *Dimetrodon* increased in body size throughout the Early Permian and specialized into an apex predator niche in a novel terrestrial environment that would form the template for every terrestrial community thereafter (9, 10). Within the group, disparate dental patterns present an opportunity to evaluate biomechanical variation through experimentation in this novel terrestrial ecosystem.

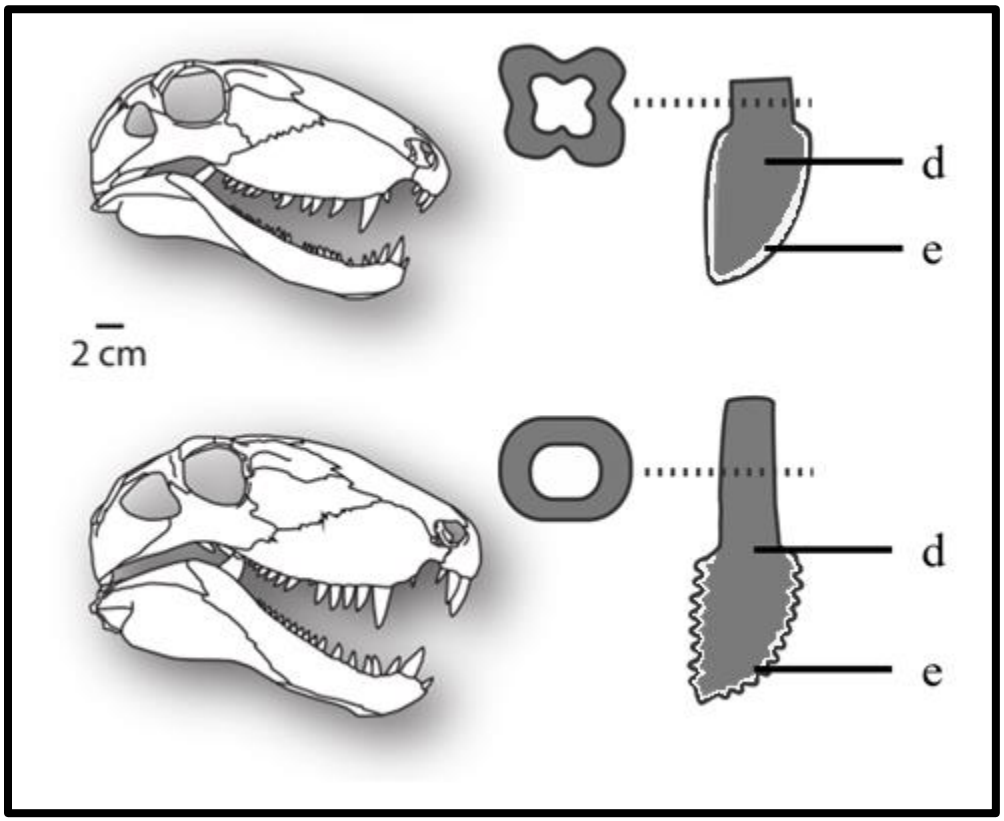

Figure 1: Illustration of Dimetrodon tooth root and crown morphology.

Above: D. milleri *with folded, short roots and smooth enamel along the carinae. Below:* D. grandis *with straight, elongated roots and denticles along the carinae. Hatched lines indicate cross-section through the tooth roots. Dark grey indicates dentine and light grey indicates enamel. Legend d, dentine; e, enamel. Figure modified from Brink et al 2014.*

Structural mechanical methods may be used to elucidate functional variation in vertebrate dentitions. Finite element analysis (FEA) is a digital modelling technique used to predict how structures like teeth will react to various forces without damaging the original objects. This process involves digitization of a fossil specimen to create complex morphologies represented by thousands of interconnected nodes, with assigned material properties of modelled tissues (11). These biological simulations can be used to examine the vulnerability of bone to tension, compression, and torsion, providing ecological insight from morphological differentiation into the drivers of evolutionary change (12). Models can be constructed in either two or three dimensions, with strengths and weaknesses for both methods (13). Teeth are non-homogenous, consisting of a central pulp interspersed with blood vessels, surrounded by a thick dentine layer and finally a cap of hard enamel. Within paleontological dental modelling, a single material type is often used to maintain model simplicity despite knowing the influence of variable material properties (14-16). To accurately examine tooth function in *Dimetrodon* with regards to root morphology and carinae with and without denticles, assignments of respectively different tissue material properties are necessary. These tissues [dentine, enamel, alveolar bone, and cortical bone] vary in their material properties and distribution which dictate how they react to an applied force.

In this study, we set out to answer the following questions:

1) Compared to smooth carinae, how do denticles alter the biomechanical performance of the dentition of *Dimetrodon*?
2) What are the biomechanical differences between a plicidentine root and the derived elongated, smooth roots within *Dimetrodon*?

Virtual experimentation will help us determine whether changes in dental microstructure and morphology led to changes in overall efficiency and tooth function in *Dimetrodon* during the establishment of the first modern-type terrestrial ecosystems.

Methods and Methods

Specimens were CT scanned and then processed in ImageJ before being segmented using Amira 3D Version 2021.1 from Thermofischer Scientific. A full skull of *Dimetrodon incisivus,* MCZ-VPRA-2779 and a maxilla of *D. borealis* ANSP-9524 were scanned at Princess Margaret Hospital, Toronto, Canada using a Toshiba Aquilion One. Scan parameters were set at 135 kVp and 500mA with an exposure time of 3000 ms.. Both specimens were reconstructed at a voxel size of 1 x 1 x 1mm.

This study uses a combination of 2D and 3D modelling of *Dimetrodon* teeth. 2D models were drawn in Adobe Illustrator Version 24.3 from a series of thin sections, CT, photographs, and the literature for two species: *Dimetrodon milleri* and *D. borealis*. Cross-sectional images were assigned to a separate layer, allowing images to be overlain with moderate transparency. Enamel, dentine, alveolar bone, and cortical bone were each constructed as separate, mutually appressed closed polygons for their entire continuous cross section.

2D FEA was performed in COMSOL Multiphysics Software version 5.5. Algorithm-based auto-meshing was used to fill the tissue polygons while preserving the surface mesh. This retained the manual nodes between tissue boundaries, allowing tissue layers to directly interact with adjacent systems. Anatomically relevant material properties are listed in Table 1.

Two separate 2D conditions were examined with structurally different models, drawn perpendicularly both mesio-distally along the carinae and labio-lingually. The first series examined the structural role of enamel and dentine along the carinae. Both denticulate and non-serrated carinae were reconstructed on the same root structure and dentine frame. The plane of choice was along the mesio-distal carinae of the tooth where the enamel is thickest. *Dimetrodon milleri* was modelled to contain a uniform 0.3mm enamel layer, representing the thickening along the carinae. The carinae of *D. borealis* contain denticles, which vary in size depending on the sinuosity of the carina. The thinnest enamel troughs were at a minimum 0.1mm whereas the thickest measured 0.2mm. Each denticle was constructed to be unique from the adjacent denticles. A 1000N force applied directly on the tooth tip in the z-axis was used to simulate directly biting down on a food item. This is a reasonable value given the size of *Dimetrodon*, serving our goal of interpreting stress distributions independent of force magnitude (17). Nevertheless, we can calculate stress and strain magnitudes at other forces because under our linear assumptions, stress and strain scale linearly with force.

A separate set of models was created to examine the influence of different root folding and lengths. Transverse, labio-lingual 2D cross-sections were created to evaluate

the different biomechanical influences between long and short roots. To decrease model complexity, smooth enamel was used for each, and the root was treated as straight with no plicidentine folding. This created a useful hypothetical condition of long roots with a smooth crown. A 1000N force was applied at a 70° angle to nodes at the tooth tip to emulate prey struggle and add a lateral component to this simulation.

3D Model Design

The 3D models were created from the segmentation of two specimens, the complete skull of MCZ-VPRA-2779, *D. incisivus*, and ANSP 9524 a *D. borealis* maxilla. The largest caniniform tooth was segmented using Amira with neighboring alveolar bone and a wedge of cortical bone from the host maxilla. The dentine, alveolar bone, and cortical bone were segmented individually and given material properties as seen in Table 1. The models were given fixed boundaries along their flat surfaces and treated as an isotropic system. A downwards force of 4000N was directed at 20 adjacent nodes radiating from the tooth tip to replicate masticatory forces.

Dental Tissue	**Density (G /cm)**	**Young's Modulus**	**Poisson's ratio**	**Presented In:**
Alveolar bone	0.80	9.0x10^3	0.31	(15) Winter et al., 2011
Cortical bone	1.90	1.1x10^4	0.30	(13) Romeed et al., 2006

Dentine	2.14	1.8x10^4	0.31	(13) Romeed et al., 2006
Enamel	2.50	6.0x10^4	0.31	(18) Enax et al., 2013

Table 1: Material properties of dental tissues obtained from the literature.

Results

Tooth crown serrations

Figures 3-6 examine the behavior of the tissues along the mesio-distal axis in the crown (Figs. 3 and 4) and in the root (Figs. 5 and 6). In the first simulation, a 1000N force was initially applied directly to nodes along the tooth tip to replicate the highest stress concentration condition, the initial puncture into prey (Fig. 2,3).

The overall pattern evident in the smooth enamel is the gradation of stress and strain. High concentrations of stress travel across the smooth enamel surface, crossing the enamel-dentine junction primarily at the location of force application (Fig 2). Both first and third principal strain (tensile and compressive strain, respectively) concentrate on the distal side of the tooth, with third principal strain concentrating higher and around the tooth tip. The enamel and dentine buffer the majority of force before it reaches the root.

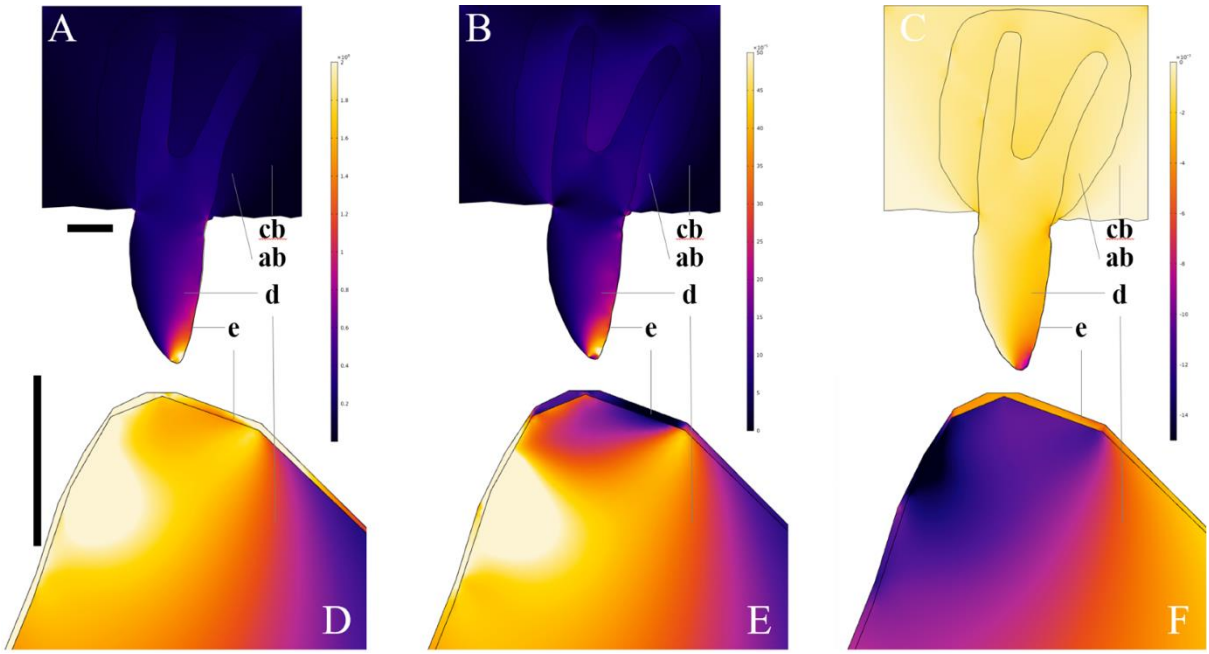

Figure 2: Results of a hypothetical caniniform smooth-enameled tooth with deep roots subjected to an applied 1000N vertical force

Distributions for a) & d) von Mises stress b) & e) first principal strain c) & f) third principal strain. To reveal gradations of magnitude maximum visualized stress set to 200MPa, and strains at 0.15 and –0.15, respectively. Legend: ab, alveolar bone; cb, cortical bone; d, dentine; e, enamel. Scale bar for 2a) b) c) = 0.5 cm and for d) e) f) = 0.25 cm.

In the second simulation, the 1000N force was applied to a tooth with denticles (Fig. 3). Loads applied on the denticles concentrated energy between the denticles. Gradation is present but in smaller overall areas, resulting in the localization of stress and strain energies. Stress and strain are low on the outer surfaces of the denticles. Stress values in the dentine are lower than in the smooth enamel condition. Overall stress and strain are again buffered before reaching the root.

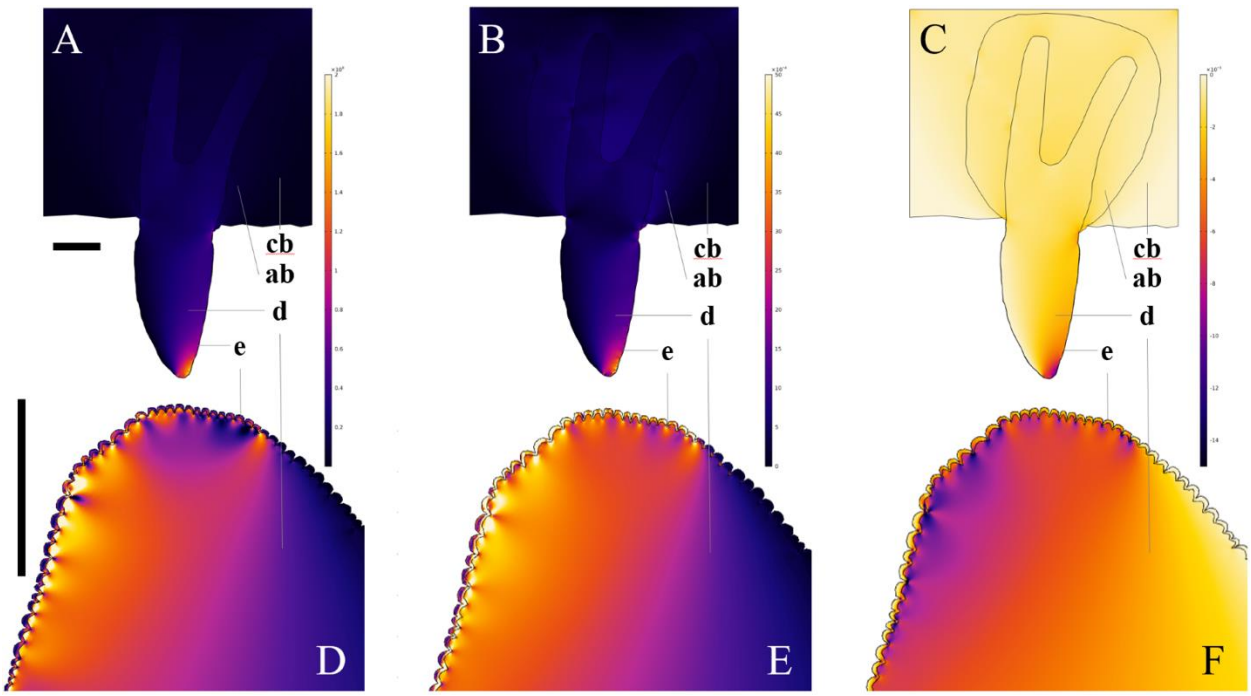

Figure 3: Results of a caniniform tooth with denticles subjected to an applied 1000N vertical force

Distributions for a) & d) von Mises stress b) & e) first principal strain c) & f) third principal strain. To reveal gradations of magnitude maximum visualized stress set to 200MPa, and strains at 0.15 and –0.15, respectively Legend: ab, alveolar bone; cb, cortical bone; d, dentine; e, enamel. Scale bar for 2a) b) c) = 0.5 cm and for d) e) f) = 0.25 cm.

Tooth root length

Models were created in a transverse (labio-lingual) plane to examine the performance of the two different root lengths and tooth attachment styles. The ancestral, short root teeth had a 2000N force applied at a 70° angle to the tooth tip. This was accomplished by applying two component vectors on the labial edge of the tooth apex (Fig. 4,5).

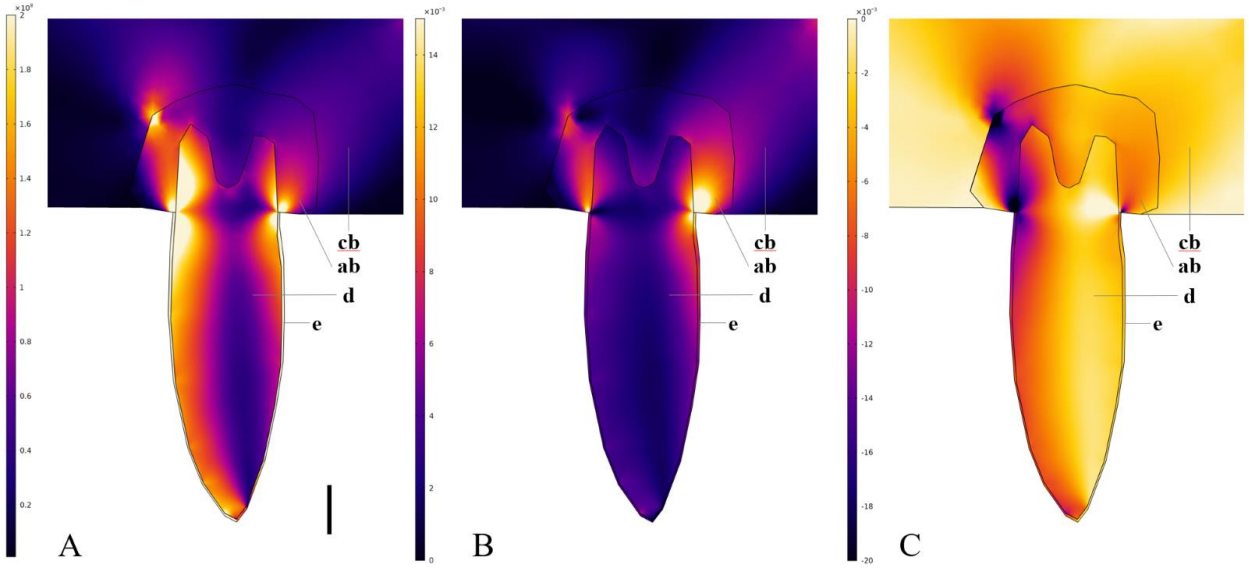

Figure 4: Results of a transverse short root subjected to an applied 2000N force at an angle of 70°

Distributions for a) von Mises stress b) first principal strain c) third principal strain. To reveal gradations of magnitude maximum visualized stress set to 200MPa, and strains at 0.15 and –0.15, respectively. Legend: ab, alveolar bone; cb, cortical bone; d, dentine; e, enamel. Scale bar 0.5 cm.

In the short root (Fig 4), stress and strain are concentrated on the opposite edge at the interface between the crown and root. Strain energy was concentrated along the peripheries of the dentine and enamel, with low energies present in the core of the tooth. Both stress and strain are transmitted primarily through the alveolar bone along this vector direction, with a similar but less extensively radiating pattern occurring perpendicularly on the same side as force application. These then grade through the cortical bone. Applying the force at an angle increased the tensile strains on the leading edge, giving an interesting and consistent distribution of the first principal strain along the labial edge leading from the jawbone. Compressive deformation was opposed, primarily concentrating on the lingual edge of the dentine and alveolar bone.

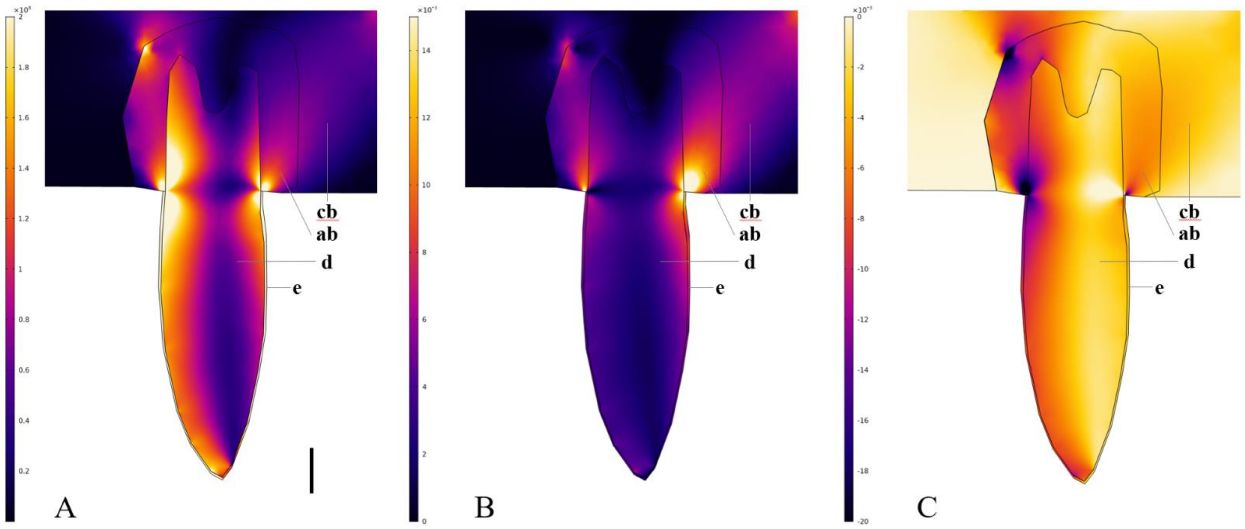

Figure 5: Results of a transverse long root subjected to an applied 2000N force at an angle of 70°

Distributions for a) von Mises stress b) first principal strain c) third principal strain. To reveal gradations of magnitude maximum visualized stress set to 200MPa, and strains at 0.15 and –0.15, respectively. Legend: ab, alveolar bone; cb, cortical bone; d, dentine; e, enamel. Scale bar 0.5 cm.

The pattern in the deeper root appears similar to that of the short root, with high values along the vector of force application through the root as well as perpendicularly (Fig 5). Higher stress values are retained in the dentine root component. Stress and strain are reduced entering the alveolar bone and subsequently the cortical bone. Stress and strain appear to be directed through the root from the boundary between the root and the crown, with the root experiencing notable stress. Energy does not appear to primarily be transmitted from the sides of the root to the alveolar bone, concentrating at the deepest extent of the root.

Tooth Root Morphology

To evaluate the influence of root shape, 3D models were subjected to a 4000N force directed along principal axis x onto the tooth tip (Figs 6 and 7). Examining the root structure in 3D showed slight variations in the distribution of stress and strain values

between morphologies. Both models were deformed and bent mesio-distally when subjected to an applied force. The degree of bending appeared to vary depending on the alveolar bone extent which compensated for this action. Greater levels of perpendicular deformation were seen in *D. borealis*. In both specimens, the highest forces were seen in the dentine, with a fraction passing forward to the alveolar bone, typically along the carinal planes in the mesio-distal direction. This then does not propagate beyond the tissue level, limiting the force experienced to slight variations in local distributions.

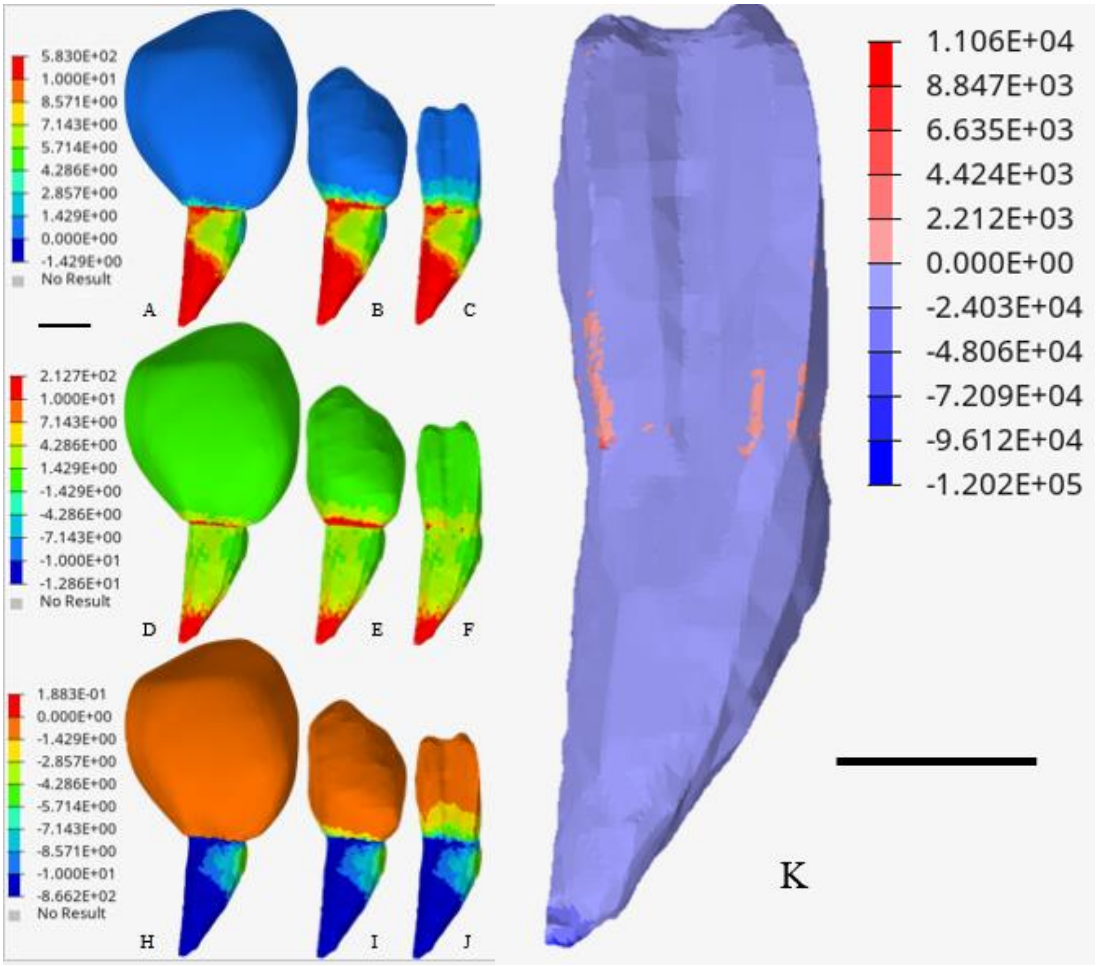

Figure 6: 3D finite element results of a folded root subjected to an applied 4000N force at the tooth tip.

Full model on the left, alveolar bone and crown in the middle, and crown only on the right for: A-C) Von Mises stress distribution capped at 1000MPa, D-F) First Principal Strain maximum 500, and G-I) Third Principal Strain maximum -500 in a. K) Von Mises uncapped on crown. Scale bar 1 cm.

Figure 6 shows the propagation of energy through a folded plicidentine root with surrounding alveolar and cortical bone. Surrounding the folded root again is alveolar bone of variable thickness extending between undulations to form a smooth outer surface. A uniform layer of cortical bone surrounds this alveolar bone to create a socket the tooth rests in. Stress extends along both the mesial and distal carinae, whereas first principal strain extends mesially, and third principal extends distally. As seen in the 2D experiments, stress and strain peak at the boundary between the crown and root to be transmitted to the alveolar bone. Figure 6K shows the dentine in isolation from the surrounding tissues to highlight the concentration of stress at the interface and along the apex of ridges in the plicidentine tooth.

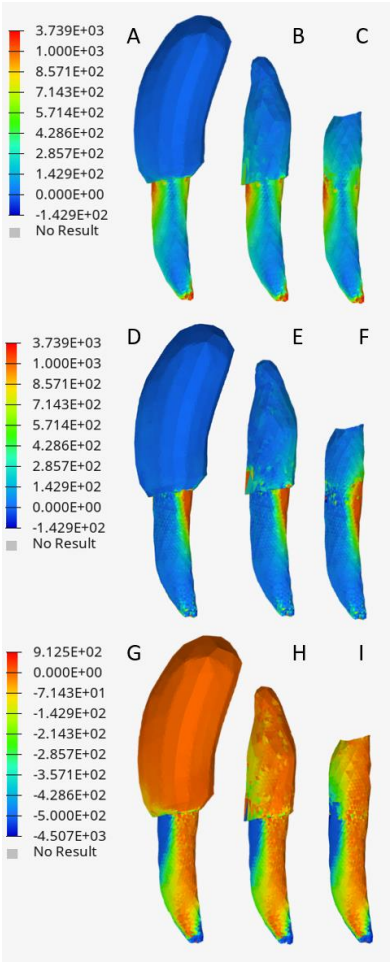

Figure 7: 3D finite element results of a smooth elongated root subjected to an applied 4000N force at the tooth tip.

Full model on the left, alveolar bone and crown in the middle, and crown only on the right for: A-C) Von Mises stress distribution capped at 1000MPa, D-F) First Principal Strain maximum 500, and G-I) Third Principal Strain maximum -500 in a. Scale bar 1 cm.

Figure 7 shows the results of the repeated experiment instead with elongate straight roots. The root is the same length as the crown, again surrounded by a layer of alveolar and cortical bone. Patterns follow those of the plicidentine tooth (Figure 6), with less overall emphasis on the carinae. High stress and strain energies persist at the boundary between the crown and the root. In both conditions the energies are effectively buffered before reaching the outer surface of the cortical bone.

Discussion

While deeply socketed blade-like teeth are shared across multiple hypercarnivorous groups, they occur for the first time in *Dimetrodon*. Within this genus is a transition from the ancestral condition of roots with plicidentine and crowns with smooth carinae to a derived tooth attachment structure and ziphodont tooth crowns. This variation frames *Dimetrodon* as an interesting taxon to focus our study, especially given the surrounding environmental context of this transition in the first modern-type terrestrial ecosystems in the Early Permian.

For the tooth crown analyses, the enamel played a significant role in both conditions in terms of von Mises stress. Rather than transferring energy directly to the dentine, a portion of the energy was contained in the enamel and deflected across the surface of the tooth. This was more apparent on the distal side as the steeper angle facilitated direct transfer of energy. The smooth carinae (Fig. 3) saw higher stress values approaching 200MPa over a greater area of the dentine than what was seen in the denticulate condition (Fig. 4). A shallow gradient appeared, with most of the energy located towards the distal edge of the tooth. In contrast, the denticulate teeth saw these same values over a much smaller area. An alternating pattern of exceedingly high stress and strain appears in the trough between the enamel-capped denticles. This would indicate concentrated areas of high stress, and lead to the localization of stress factors. A similar less pronounced pattern is also present when examining both the first and third principal strains, which respectively represent primary tension and compression influence. This area between the denticles matches the position of an interdental fold in other taxa, suggesting more derived ziphodont teeth in therapsids and theropod

dinosaurs are better adapted to withstand stress and strain on the teeth. The shape of the enamel, while assisting with slicing through soft tissue, focuses energy to the bottom of the syncline in the interdental fold. The presence of globular dentine could strengthen the area against these localized forces, stopping cracks from propagating throughout the tooth (4).

Between the conditions evaluated by the transverse model, stress and strain followed a similar pattern of energy transmission with differing magnitudes. In both conditions, the alveolar bone socket performed as a buffer to compressive strain before slight amounts made their way to the surrounding jawbone. The compressive strain was much more prevalent in the short root compared to the elongate root, especially directly below the dentine core. Deep roots translated these forces deeper but of smaller relative magnitude than that of the shorter root. Buffering by the root would permit higher overall force values to be absorbed by the dentine and less experienced by the surrounding jaw. This would increase the effective force capacity of *Dimetrodon's* jaw, facilitating higher bite forces. This morphology may have been an adaptation in response to the greater size in derived members, and a compensation for greater loads during mastication (2).

The 3D models examined the transmission of forces through the crown and root with slight variations in both of their morphologies. In the broader respect, at these forces there is not an appreciable difference in force output to the cortical bone. Despite the folding in the root of the plicidentine tooth, localizations through the alveolar bone did not occur, resulting in harmonious force distributions to the rest of the skull between the models. Surface area differs by 1% between the two conditions, supporting previous

suggestions that plicidentine increases surface area for better attaching teeth to the jaw (7). Smooth roots that extend further into the maxilla, simplifies the overall topological structure, and allows for a more even distribution of forces without focusing localized stresses into the apices of the roots. This may have also been a slight adaptation to minimize the collateral damage of tooth replacement. Overprinting from the ankylosis of a functional tooth may have eroded the attachment of neighboring tooth positions. A different attachment style may have increased tooth longevity, decreasing the metabolic cost from replacement.

These models are not a perfect 1:1 recreation of *Dimetrodon* dentition. As seen in Table 1, enamel values were derived from those acquired from human and crocodilian values. This introduces potential error as we have no extant data for the biomechanical performance of *Dimetrodon* enamel. *Dimetrodon,* among many of its contemporaries, possessed a tissue termed Synapsid Columnar Enamel (19). The performance in vivo of this tissue is difficult to assess barring the development of lab grown synthetic material, as its structure differs with any known extant enamel. More prosaic cementum is visible in histological sections as a thin tissue between the dentine and alveolar bone in the tooth root. This arrangement serves as the actual site of attachment between the tooth root and the rest of the jaw. This tissue was not modelled because of the overall thinness, <0.5 mm; being comparable to a portion of the enamel thickness which already is quite small on this model. While the properties and importance of enamel are well known, the performance of cementum based on extant specimens is lacking and would be difficult to best replicate without a dedicated study into its biomechanical influence. While

Dimetrodon is a mammalian predecessor, it did not retain a mammal-like periodontal ligament throughout the life of each tooth, and teeth were ankylosed to the jawbone (20).

This study focused on the extremes of *Dimetrodon* dental diversity despite an overall gradational morphological history within the taxon. The smooth enamel of *D. milleri* was directly compared to the microstructure present in the denticles of *D. grandis* or *D. borealis*. Some species such as *D. limbatus (D. incisivus)* have teeth with enamel-only serrations without a dentine core (1). While not modeled in this instance, we expect a disruptive pattern to remain in the enamel, from the irregular shaped denticles and a moderate condition in the dentine with localized, but broader distributions from a smooth enamel-dentine junction.

Teeth are excellent indicators of diet and are often, as in mammals, the primary remains preserved in the fossil record that can help interpret paleoecologies of extinct animals. Changing tooth morphologies with biomechanical significance indicates a dietary shift signaled by these stress and strain patterns. Perhaps this shift in tooth morphology is a response to the broader ecosystem changes occurring in the Permian at this time (9,10). For the first time on land, large-bodied herbivores such as caseids and edaphosaurids were a potential new prey item for *Dimetrodon*. Compared to the flattened bodies of amphibians like *Diplocaulus* or *Zatrachys*, these large-bodied herbivores likely had fleshier bodies (21). While the denticles may have been weaker when subjected to repeated stress events or performed worse at comminution of bone, serrations have been shown to aid in the processing of large sections of soft tissue (2). This effectiveness at soft-tissue processing in derived species of *Dimetrodon* raises parallels with carnivorous

dinosaurs. Compared to extant mammal communities, the low rates of dinosaur bone with bite marks have been used to suggest minimal scavenging (22). Similarly, little evidence from these Early Permian communities supports this behaviour in *Dimetrodon* suggesting active predation. This trade-off of potentially reducing the functional life span from fracturing and wear may have been worthwhile if it aided in the consumption of large-bodied prey and reduced interspecific predation competition.

Conclusion

The modelled tooth structures in these simulations did not perform as a homogenous unit, instead, complex patterns emerged from the heterogenous material properties and morphology of the teeth. The elongate tooth root shared a similar pattern to its short counterpart but was able to distribute energy over a greater area, reducing the impact on the surrounding bone by all metrics. A folded tooth root localized stress at the apex of fold crests in all axes when subjected to a perpendicular force. The morphology of the root has little impact on the surrounding tissue at regular force intervals. Denticles experienced more stress than seen in the straight enamel simulation at the cost of creating a more localized and disruptive pattern in the dentine between denticles. The denticles of derived species of *Dimetrodon* were more susceptible to damage from high kinetic energies but offered benefits to the animal in terms of prey processing. This suggests increased consumption of prey with thick layers of soft tissue.

References

1.Brink KS, Reisz RR. Hidden dental diversity in the oldest terrestrial apex predator *Dimetrodon*. Nature Communications. 2014 May ;5(1).

2. Abler WL. The Serrated Teeth of Tyrannosaurid Dinosaurs, and Biting Structures in Other Animals. Paleobiology. 1992;18(2):161–83.

3. Brink KS, Reisz RR, LeBlanc ARH, Chang RS, Lee YC, Chiang CC, et al. Developmental and evolutionary novelty in the serrated teeth of theropod dinosaurs. Scientific Reports. 2015 Jul 28;5(1):1–12.

4. Whitney MR, LeBlanc ARH, Reynolds AR, Brink KS. Convergent dental adaptations in the serrations of hypercarnivorous synapsids and dinosaurs. Biol Lett. 2020 Dec;16(12):20200750.

5. Maxwell EE, Caldwell MW, Lamoureux DO. The structure and phylogenetic distribution of amniote plicidentine. Journal of Vertebrate Paleontology. 2011 May 1;31(3):553–61.

6. MacDougall MJ, LeBlanc ARH, Reisz RR. Plicidentine in the Early Permian Parareptile *Colobomycter pholeter*, and Its Phylogenetic and Functional Significance among Coeval Members of the Clade. PLOS ONE. 2014 May 7;9(5):e96559.

7. Brink KS, LeBlanc ARH, Reisz RR. First record of plicidentine in Synapsida and patterns of tooth root shape change in Early Permian sphenacodontians. Naturwissenschaften. 2014 Nov;101(11):883–92.

8. Pearson MR, Benson RBJ, Upchurch P, Fröbisch J, Kammerer CF. Reconstructing the diversity of early terrestrial herbivorous tetrapods. Palaeogeography, Palaeoclimatology, Palaeoecology. 2013 Feb;372:42–9.

9. Brocklehurst N, Brink KS. Selection towards larger body size in both herbivorous and carnivorous synapsids during the Carboniferous. Clemente CJ, editor. FACETS. 2017 May 1;2(1):68–84.

10. Olson EC. Community Evolution and the Origin of Mammals. Ecology. 1966;47(2):291–302.

11. Edelsbrunner H, Mucke EP. Three-Dimensional Alpha Shapes. ACM Transactions on Graphics. 1994 Jan;13(1):30.

12. Moreno K, Wroe S, Clausen P, McHenry C, D'Amore DC, Rayfield EJ, et al. Cranial performance in the Komodo dragon (*Varanus komodoensis*) as revealed by high-resolution 3-D finite element analysis. Journal of Anatomy. 2008;212(6):736–46.

13. Romeed SA, Fok SL, Wilson NHF. A comparison of 2D and 3D finite element analysis of a restored tooth. Journal of Oral Rehabilitation. 2006 Mar;33(3):209–15.

14. Peterson J, Dechow PC. Material properties of the human cranial vault and zygoma. The Anatomical Record. 2003;274A(1):785–97.

15. Winter W, Krafft T, Steinmann P, Karl M. Quality of alveolar bone — Structure-dependent material properties and design of a novel measurement technique. Journal of the Mechanical Behavior of Biomedical Materials. 2011 May 1;4(4):541–8.

16. Herbst EC, Lautenschlager S, Bastiaans D, Miedema F, Scheyer TM. Modeling tooth enamel in FEA comparisons of skulls: Comparing common simplifications with biologically realistic models. iScience. 2021 Nov;24(11):103182.

17. Sakamoto M. Assessing bite force estimates in extinct mammals and archosaurs using phylogenetic predictions. Porro L, editor. Palaeontology. 2021 Sep;64(5):743–53.

18. Enax J, Fabritius HO, Rack A, Prymak O, Raabe D, Epple M. Characterization of crocodile teeth: Correlation of composition, microstructure, and hardness. Journal of Structural Biology. 2013 Nov 1;184(2):155–63.

19. Sander PM. Non-mammalian synapsid enamel and the origin of mammalian enamel prisms: The bottom-up perspective. In: Koenigswald W v., Sander PM, editors. Tooth Enamel Microstructure. 1st ed. CRC Press; 1997. p. 41–62.

20. LeBlanc ARH, Brink KS, Whitney MR, Abdala F, Reisz RR. Dental ontogeny in extinct synapsids reveals a complex evolutionary history of the mammalian tooth attachment system. Proceedings of the Royal Society B: Biological Sciences. 2018 Nov 7;285(1890):20181792.

21. Romer AS, Price LW. Review of the Pelycosauria. Geological Society of America; 1940. 596 p.

22. Fiorillo AR. Prey bone utilization by predatory dinosaurs. Palaeogeography, Palaeoclimatology, Palaeoecology. 1991 Dec;88(3–4):157–66.

Chapter 3: MODELING JAW ADDUCTION IN THE NON-MAMMALIAN SYNAPSID *DIMETRODON* USING MULTI-BODY DYNAMICS ANALYSIS AND FINITE ELEMENT ANALYSIS

Formatted to the style of Journal of Anatomy

https://onlinelibrary.wiley.com/page/journal/14697580/homepage/forauthors.html

Abstract

The most renowned predator of the Early Permian, *Dimetrodon* (Synapsida: Sphenacodontidae), evolved as members of a novel, amniote-dominated terrestrial landscape. Previous reconstructions of *Dimetrodon* jaw musculature encompassed reptilian and mammalian styles. Since the last of these reconstructions, seminal works in the subfield of biomechanics have revolutionized our understanding of the feeding apparatus and muscle reconstructions. In this study, we use a virtual skull of *Dimetrodon incisivus* to create three alternate models of the early synapsid feeding apparatus and compare their muscle forces, rotational kinetic energies, and bite force at the teeth. 3D muscles are built to spatial limitations from the skull and areas of attachments on the virtual skull to determine physiological cross-sectional area and inform individual force values. We found that general taxon bite force estimates based on body size and skull height underestimate the bite force of *Dimetrodon*. A modification of the traditional dry skull method used in reptiles comparatively underestimates the values returned from our muscle reconstructions. Multi-body dynamics analysis is used to determine bilateral muscle system output as forces loaded onto prominent heterodont teeth for finite

element analysis. Preferential stress and strain thresholds for the caniniform teeth of *Dimetrodon* amid a heterodont dentition furthers an expected role of this animal as apex predators of the Permian. *Dimetrodon* would have been the first animal to produce bite forces capable of bringing down emerging large-bodied herbivores, with significant implications for the origin of stem-mammalian feeding complexes as well as the establishment of terrestrial ecological communities.

Introduction

The Early Permian (295-270MA) is a unique period in Earth history documenting the establishment of modern, amniote-dominated terrestrial ecosystems (Olson 1966; Pearson et al., 2013; Huttenlocker et al., 2021). The largest predators of this time were the famously sail-backed sphenacodontid synapsids, *Dimetrodon*. In a period of about ~20 million years, this animal demonstrates the evolutionary trend shared across many Permian tetrapods, increasing in gross body size to capitalize on emergent niches and diets (Brocklehurst and Brink, 2017). *Dimetrodon* has both wide distribution and high prevalence at Early Permian localities across North America and Europe, being present across a variety of extinct communities (Brink and Reisz, 2012; Brocklehurst et al., 2017).

Dimetrodon rapidly populated the post-Carboniferous terrestrial ecosystem, appearing as a cosmopolitan predator (Case, 1904; Brocklehurst et al., 2018). Their skull supported a new line of action for an external adductor and a raised coronoid step to differentiate them from the most primitive synapsids (DeMar and Barghusen,1972). Elsewise, *Dimetrodon* skull morphology was established early in its evolutionary history, with little morphological change as the group increased in size and varied their dentition

(Romer and Price, 1940; Brink and Reisz, 2014; Brink et al. 2014). Three separate dental suites are represented by *Dimetrodon incisivus:* 1) peg-like incisiform teeth on the premaxilla 2) teardrop-shaped, large caniniform teeth posterior to the diastema on the maxilla and 3) posteriorly diminutive caniniform cheek teeth. Interestingly, these dental characteristics become further modified in derived members of *Dimetrodon* while their overall cranial morphology has remained relatively constant (Romer and Price, 1940; Reisz, 1987). The conserved skull morphology of *Dimetrodon* suggests that musculature might be minimally variable between species.

While preserved instances of vertebrate soft tissues and musculature are exceedingly rare, clues such as muscle scarring or broader phylogenetic homology inform architecture. Cranial muscle topology is especially interesting for taxa such as *Dimetrodon,* which occupy a critical position at the earliest offshoot of stem mammals from proto-reptiles and the fork between two muscle topologies (Jones et al., 2009). One major osteological difference between mammals and other amniotes is the incorporation of the articular and quadrate bones into the ear, necessitating a change in the musculature and jaw architecture. *Dimetrodon* maintains a reptilian hinge system at its tempoolmandibular joint (TMJ) but how this extends to the adductor musculature is contentious. Muscle topologies rely on numerous considerations, including the primitive condition, evidence of bone remodification from muscle action, extant dissections, and physical constraints from the skull morphology and other tissues (Crompton and Parkyn, 1963). Different reconstructions through the 20th century based on the same skull morphology have produced different musculature patterns resembling para-reptilian,

rhynchocephalian, and proto-mammalian influences (Watson 1948; Fox 1964; Barghusen 1973). These different muscle topologies alter key adductor muscles' position, size, angle, and attachment locations. Even slight changes to muscle reconstruction can have significant implications on the performance of the apparatus (Broyde et al., 2021). The cranial anatomy can support all three topologies, so we must find a separate test for our hypotheses.

One course of evaluation for these muscle reconstructions is model analysis, to justify our theories with mechanical fitness. Biomechanically, muscle efficiency may be only one influence of thousands on the evolution of an organism, but it is one that can be quantifiably examined. Each muscle topology consists of different muscle arrangements in relation to the skull, resulting in different sizes and action angles. Each reconstruction will facilitate the calculation of the total muscle forces onto the mandible of *Dimetrodon* at different efficiencies. The style that is then the most efficient at creating a bite force in the skull would be favoured for mastication and is therefore the most biomechanically supported (Rudwick 1964). To determine the cumulative force imparted by the muscles on the jaw, multi-body dynamic analysis (MDA) will be employed to accurately model the kinematic movements on the skull architecture. Efficiency can then be examined against related ‘risky’ models, in this case, the older rhynchocephalian and mammalian models, to see how performance differs between the three. Beyond just testing one model, by having multiple anatomically valid constructions we can further increase our confidence in the contemporary ‘reptilian’-style of musculature. If the older models perform as well

or better than our current paradigm, then our modern reconstruction is not biomechanically supported and needs to be re-evaluated.

A convenient coincidence of this test is that by evaluating the bite force component of these musculature systems, we will produce a maximum bite force achievable between three competing adductor muscle topologies. This estimation can then be used for finite element analysis (FEA) examination during simulated oral manipulation of prey. How stress and strain energies are transmitted through the skull is dependent on the morphology present, specifically during a maximum load biting series. Finally, by isolating these forces onto specific tooth types we can see how the skull may be adapted for maximizing the efficiency of the heterodont dentition. Specific adaptations of the teeth as seen in extant and extinct taxa can then be used to inform inferences relating to apparent ecological niche.

Methods

CT scans

Two *Dimetrodon* skulls were digitized through computed tomography (CT) scanning to accurately create three-dimensional models. MCZ-VPRA-2779 is a complete articulated *Dimetrodon incisivus* skull, scanned at Princess Margaret Hospital at 1mm x 1mm x 1mm voxel resolution. FPDM-V-9671 is a fragmentary skull with parietal, maxillary and mandibular elements CT scanned in Tokyo, Japan, at 1mm x 1mm x 1mm voxel resolution. Initial surface visualization was completed in AMIRA 3D version 2021.1, with each model being exported as .stl files. These were then placed together in BLENDER version 3.2.1 for manual remeshing and nodal clean-up of the triangular surface mesh. The proportions of FPDM-V-9671, as well as literature values, informed the

retrodeformation of MCZ-VPRA-2779. The internal braincase, including the basisphenoid, was modelled based on illustrations of *Dimetrodon* and intact 3D models of other early synapsids (Romer and Price, 1940; Brink and Reisz, 2012). The mandible was modelled as 3 293 258 triangles and the cranium 358 340, increasing complexity towards the posteroventral part of the meshes. Once the mesh quality was acceptable, the skull model was converted into a rigid body Parasolid for MDA (Multibody Dynamic Analysis) in ADAMs 2021 from MSC Software.

Muscle reconstruction

Muscle construction was adapted from a process detailed in Broyde et al. 2021. Each muscle was constructed from 5 circle meshes of 32 vertices. These were positioned equidistantly from each other and manipulated internally to fit the shape of the muscle head. Slight variations in the distances were used to match the folding of certain muscle groups accurately. The bridge edge loop process was then applied to create a volumetric construction of the muscle fibres. This process was repeated for three different muscle topologies.

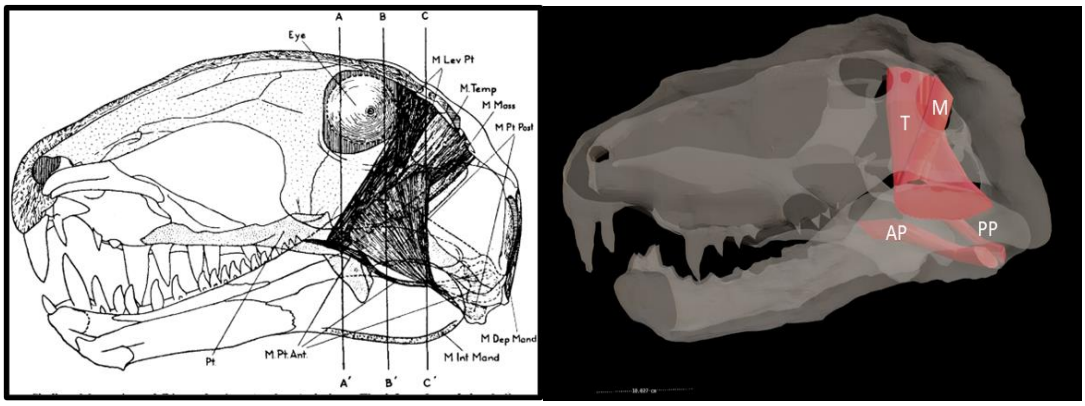

Fig 1:Proto-mammalian muscle topology

Left) 2D reference from Watson 1948 Right) virtual 3D reconstruction. Abbreviations: AP, anterior pterygoid group; M, masseter group; T, temporalis group; PP, posterior pterygoid group.

The first muscle topology (Fig 1) is based on Watson's (1948) Early Synapsid muscle system description. Heavily influenced by later mammalian patterns, this adductor system is split into four muscle heads: the masseter, temporalis, and anterior and posterior pterygoids. The masseter originates from a powerful tubercle on the jugal before extending a short distance to insert into a depression of the lateral dentary. The temporalis muscle inserts from an origin on the parietal on a dorsomedial section of the coronoid process. The anterior pterygoid muscle originates on the dorsal pterygoid and inserted below the reflected lamina of the angular. Finally, the posterior pterygoid originated on the epipterygoid before inserting on a rugosity of the articular.

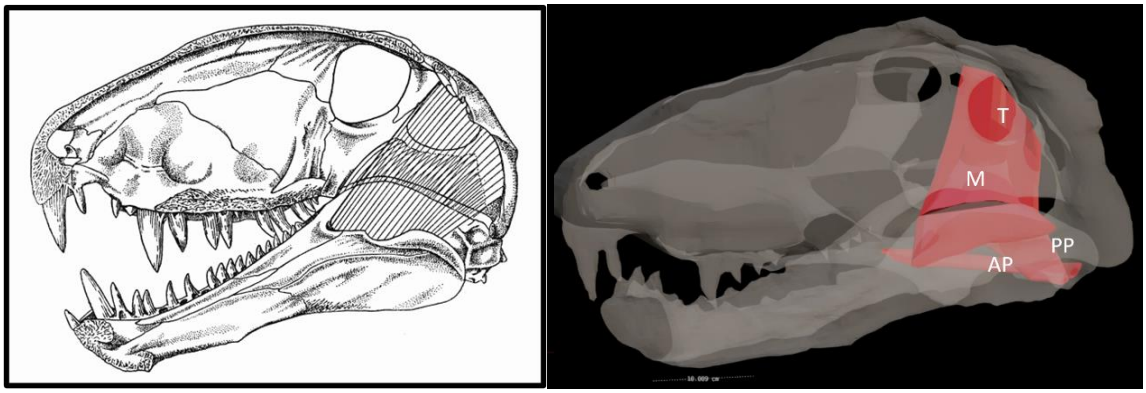

Fig 2:Rhynchocephalian muscle topology

Left) 2D reference from Fox 1964, modified from Romer and Price, 1940 Right) virtual 3D reconstruction. Abbreviations: AP, anterior pterygoid group; M, masseter group; T, temporalis group; PP, posterior pterygoid group.

The second reconstruction (Fig. 2) observes identical groupings of muscles to those described previously with alterations to their positions and size, with an overall pattern like extant *Sphenodon* (Jones et al., 2009). The masseter is moved further back

from the tuberosity of the jugal towards a position inferior to the temporal fenestra. The temporalis has an expansive origin from the postorbital strut, across the dorsal skull roof and bodeaponeurosis to the squamosal. The anterior pterygoid muscle originates from the dorsal pterygoid and adjacent bones to insert into the reflected lamina of the angular. Finally, the posterior pterygoid muscle originates on the quadrate wing of the pterygoid to insert adjacent to the anterior.

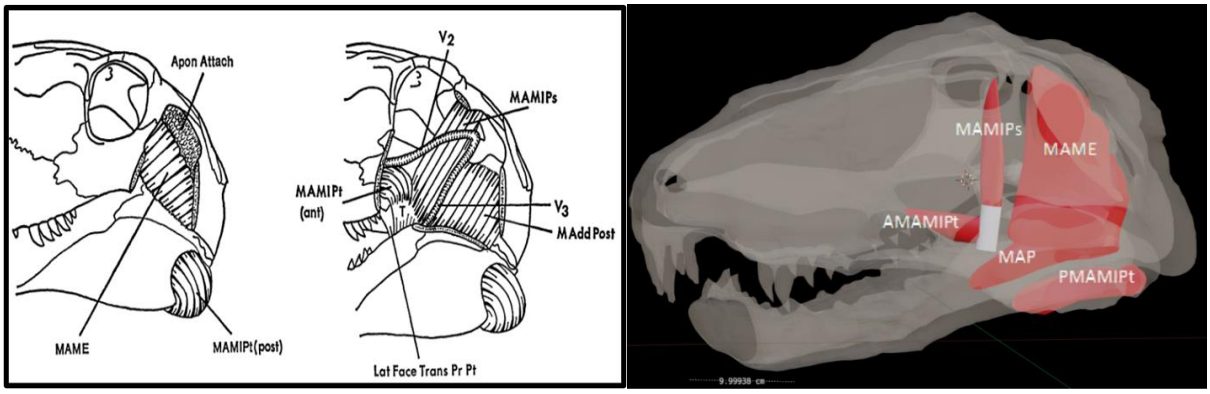

Fig 3Reptilian muscle topology

Left) 2D reference from Barghusen 1973. Right) virtual 3D reconstruction. Abbreviations: MAME, M. adductor mandibulae externus; MAP, M. Adductor Mandibulae Posterior; MAMIPs, M. adductor mandibulae internus pseudotemporalis; AMAMIPt, M. adductor mandibulae internus pterygoideus anterior; PMAMIPt, M. adductor mandibulae internus pterygoideus posterior.

For the third model, proximity to reptilians in the phylogenetic tree informed the topology (Fig 3) (Barghusen, 1973). Notably, the temporal chamber has been split between two broad muscle groups: the M. Adductor Mandibulae Externus (MAME) and the M. Adductor Mandibulae Posterior (MAP). MAME originates along the Skull Roof and lateral constraints of the chamber between the postorbital bar to the quadratojugal, inserting along the coronoid process of the dentary and surangular superior to the MAP. The MAP sits just medial to MAME, originating on the quadrate to insert into the adductor

fossa of the surangular. What would later be incorporated into the temporalis, the M. adductor mandibulae internus pseudotemporalis (MAMIPs), originates on the lateral epipterygoid and part of the parietal. MAMIPs share a tendinous origin in the anterior-most portion of the adductor fossa with M. adductor mandibulae internus pterygoideus anterior (Ant MAMIPt), which originates from the dorsal palate in the suborbital space. Finally, M. adductor mandibulae internus pterygoideus posterior (Post MAMIPt) originates from the medial pterygoid crest to insert into the lateral articular.

Each muscle was measured using the BLENDER measurement tool and object statistics to determine its length and volume. By dividing these two values, the physiological cross-sectional area could be determined and then multiplied by 300 MPa to determine the force of the muscle (Weijs and Hillen, 1985).

The pseudotemporalis and masseter force values informed the dry skull method (Thomason 1991). While initially developed for limitations provided by the zygomatic arch present in mammals, the muscle equivalencies were each used to calculate a bite force estimate through the calculation of equation 1:

Equation (1) $B_f=2(M\cdot m+P\cdot p)o$ *$Bf=2M\cdot m+P\cdot po$*

The bite force is determined by doubling the sum of two muscle products. Capitals designate the force vector, with lowercase being the lever arms of the masseter and pseudotemporalis muscles, respectively. These actions are then divided by the out-lever “o,” representing the distance from the TMJ (Temporal Mandibular Joint) to the largest tooth on the dentary.

Muscle force values were also used in the engineering software Automated Dynamic Analysis of Mechanical Systems (ADAMS) by MacNeal-Schwendler Corporation (MSC) to see how conduction of force varies with taxonomic mandible morphology. Each force vector was replicated as directed tension springs, and the line of action was averaged from the muscle recreations. There was no dampening input, and each simulation started at a gape of 30°. Tendons were assumed to apply combined muscle vectors at 100% efficiency over their attachment area. The TMJ was recreated as a revolute joint at the quadrate and articular articulation. Muscles fired maximally and synchronously on the mandible to close the entire jaw apparatus. Bone density was isometric at 1.9 g/cm^3. The maximum force was then taken at three different points along the jaw for examination.

Results

Multi-Body Dynamic Analysis

Muscle volume and length were collected from the 3D muscle models. The dry skull estimation method that utilized values for the masseter and temporalis and a measured lever arm was calculated per Equation 1. Measured and calculated results can be seen in Table 2.

Reconstruction	Muscle	Moment (N)	In lever Arm (mm)	Bite Force (N)
Reptilian	M	1899.535494	87.568	1422.165
	T	920.688476	143.714	
Rhynchocephalian	M	1637.496445	110.847	2815.1676
	T	3752.930403	109.161	
Mammalian	M	1715.292757	112.396	1200.140
	T	1113.421811	53.203	

Table 2:Force and moment results from the Dry Skull Method (Thomason 1991) applied to virtual muscle and skull for three different muscle reconstructions

Out lever was measured at 4.2 centimetres. Abbreviations: M, masseter; T, temporalis. Attachment topologies were based on original constructions by: Reptilian, Barghusen 1973; Rhynchocephalian, Fox 1964; and Mammalian, Watson 1948.

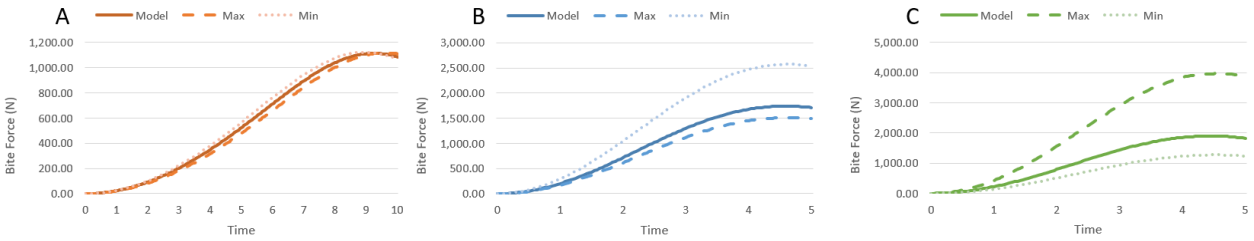

Fig 4: Impact force of the lower jaw in Newtons (N)

A) Mammalian muscle topology, B) Rhyncocephalian muscle topology, and C) Reptilian muscle topology.

Moment arms varied due to the angle of the muscle reconstructions. A temporalis lever arm of 14.4 cm is greater than the masseter in the para-reptilian topology. Conversely, the proto-mammalian system had a much greater masseter lever arm at 11.2 cm when compared to the temporalis. The rhynchocephalian lever arms were identical, 11.1 cm and 10.9 cm between the masseter and temporalis, respectively.

The pattern of lever arms did not carry over to dry skull predictions as muscle volumes comminuted them. The rhynchocephalian topology, which was calculated using the single largest muscle force of the study (temporal group 3040N), was predicted to have the most potent bite force at 2470 N. The proto-mammalian system was predicted to achieve a maximum force of 1820N. In contrast, the weakest estimate was in the para-reptilian system at 1250 N.

The results of the MDA solutions are seen as line graphs in Figs 4-6. The reptilian model resulted in 2500N mm^2 which is exactly twice what was predicted by the Dry Skull Method. The rhyncocephalian model returned a value of 1500 N mm^2 and the mammalian model 1200 N $mm^{2,}$ smaller than they were initially predicted to be.

Finite Element Analysis

Using the maximum forces obtained from MDA, we applied these forces onto heterodont tooth morphologies within the skull. In addition to the forces from jaw adduction, an additional force 25% the value of the bite force was applied laterally to determine the durability of the teeth with the incumbent stress of prey struggle.

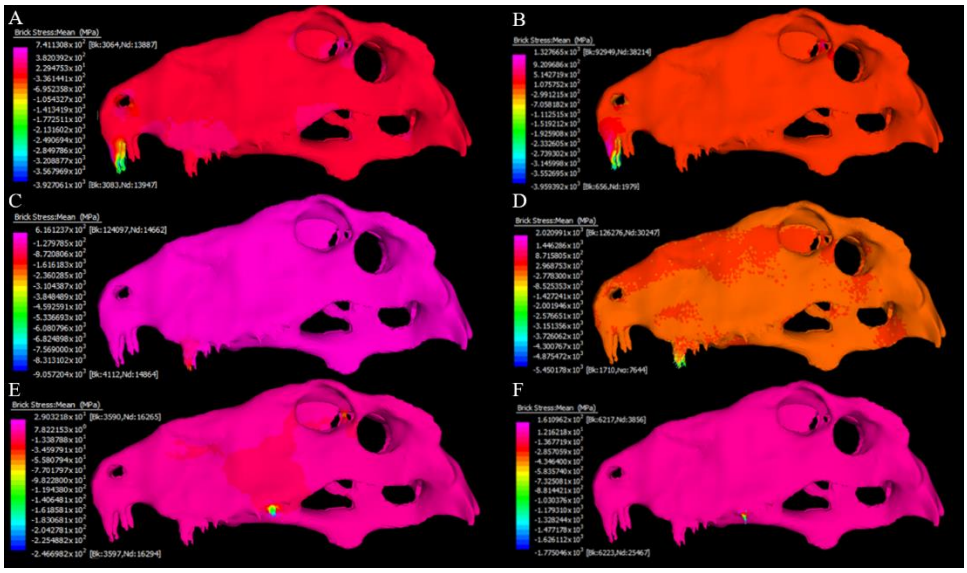

Fig 5: Average element stress of 4000N force applied to heterodont dentition

to paired incisiform a) and b) additional 1000N on the y-axis; caniniform c) and d) 1000N on the y-axis; and post-caniniform e) and f) 1000N on the y-axis;. Vector stresses available in supplementary. Results series include mean cumulative element stress, as well as stress and strain values in the xy, yz, and zx axis.

Stress and strain followed similar patterns within an axis, differentiating minimally if at all. In all conditions the yz plane experienced the highest average relative stress throughout the whole skull which is expected as these are the primary force axes.

The incisiform tooth resisted labio-lingual forces the most successfully, transmitting higher energies to the surrounding skull. The caniniform teeth distributed the highest average stress to the rest of the skull apparatus. The anterior face of the tooth experienced greater energy transmission compared to the posterior. The post-caniniform

teeth poorly dissipated stress to the maxilla and beyond, resulting in low stress seen throughout out the skull. One 4000N force was enough to cause tooth fracture in the post-caniniform tooth, unable to resist the force. This exceeds the VM stress threshold and would result in tooth fracture or even cataclysmic destruction.

Discussion

Muscle and other soft tissue reconstructions are necessary for extinct organisms, as these features of their anatomy are so rarely preserved in the geologic record. In this study, we constructed 3D models of three proposed *Dimetrodon* adductor musculature topologies to evaluate their performance efficiency. These values were then compared with other methods of bite force estimation. Examination of the different musculatures reveals an intriguing challenge in interpreting muscle scars and the morphology of the skulls. The 'correct' reconstruction is the most scientifically persuading without additional fossil finds. In truth, none of these models may accurately portray the muscle topology of *Dimetrodon* as it lived 270 million years ago without a direct line to the present; however, based on our understanding of extant anatomy and a biomechanically supported system, we have confidence in our present construction. This 3D examination lends additional visualization, and a quantitative result for each of three styles proposed.

A consideration that must be made when evaluating the performance of the jaw structure is any alternative uses. Bite force may not be a suitable vector for examining the efficiency of dextrous oral processing or specialized tooth use (Sakamoto 2021). Heterodonty indicates some form of specialization within the jaw, either for diet or environmental interactions. *Dimetrodon's* heterodont dentition can be divided into

incisiform premaxillary teeth, a single large caniniform tooth separated from the incisiform teeth by a diastema, and post caniniform cheek teeth for the rest of the maxilla. Similar ziphodont patterns are present in several taxa, both extinct and extant, with no proposed or witnessed alternative tooth use (Whitney et al., 2020). We, therefore, interpret no unexpected use of the feeding apparatus.

These functional models utilized a sculpted braincase and surrounding chondrocranium from reference material. *Dimetrodon* braincases are a rare find and consequently poorly understood. Unique features found in the braincases of some material are undetermined to be a synapomorphy for the clade or the genus (Brink and Reisz, 2012). Interspecies patterns were not the focus of this study, and beyond that, the braincase is not a structure directly adapted for the manipulation of mastication stress. The internal structure does not provide origin sites for large adductor musculature in any of the muscle reconstructions or in extant taxa. Its proximity to the feeding apparatus is a consequence of cephalization across Tetrapoda and biomechanically has never been compromised by maximal bite force. If a well-preserved braincase were to be recovered from the fossil record, it would warrant a new muscle reconstruction if the nervous pathways could be recovered.

Another assumption is that all the muscles were firing at a set of 30N/cm^2, derived from average human masticatory values despite muscle variation throughout the body (Weijs and Hillen, 1985, Buchanan 1995). This value has become close to an unlabelled standard in biomechanics, allowing for rapid comparison between different muscles and taxa. In addition, the goal of this study is to compare the performance of differing muscle

topologies and render each in three dimensions. This is also why the pennation angle for each muscle was set at 0°. Unfortunately, we have no way to access the pennation for extinct taxa without direct evidence of fibre direction. A standard solution is to calculate a series of values for maximum and minimum angles in a range. These muscle patterns are also much more difficult to compute in MDA, requiring additional processing power and time.

The dry skull method is intrinsically biased towards the power of masseter and temporalis muscles or their equivalents, skewing towards topologies that preserve these. The para-reptilian model goes as far as to split the temporal space between MAME and MAP, which further decreases the predicted strength. On the other hand, the rhynchocephalian topology expanded this temporalis group to the maximum margins afforded by the temporal vacuity. This would increase the power determined by the dry skull method. The most considerable impact, however, is likely to come from the pterygoids. All three topologies split the pterygoideus into two distinct heads, a style preserved by extant reptilians. The para-reptilian model had the greatest proportional pterygoideus strength, representing 46% of the muscle power. Watson (1948) and Fox (1964) had the pterygoids add up to 33% and 31%, respectively. All three muscle topologies presented were mapped onto the same skull with different resultant bite forces. Calculated and simulated values varied depending on the muscle architecture, which has been cited as a source of a significant error in paleontological reconstructions of bite force (Bates et al., 2021).

The three different tooth morphologies created different patterns of energy distribution through the skull architecture of *Dimetrodon*. The caniniform teeth performed the best, able to dissipate stress and strain energies homogenously throughout the skull. These teeth would be the first to impact a prey item during jaw closure and would experience the full force. From the tooth's morphology the anterior face experienced the highest stress along the carinae, whereas this was lessened on the posterior face. These high-stress areas correlate with the positions of the mesial and distal carinae on the teeth, which are areas of thickened enamel in most taxa, and denticles in derived taxa (Brink and Reisz, 2014). This also correlates with enamel wear patterns found on erupted *Dimetrodon* teeth (Brink and Reisz, 2014).

The next best performing teeth were the incisiforms, which were less successful at dissipating energy than the caniniform teeth. Stress was primarily constrained inside the tooth, localizing on the distal surfaces. Relative to the other conditions the incisiform tooth was better able to resist labio-lateral forces. This could be in part to the proximity of the midline suture between these elements. This peg-like tooth would function differently compared to the caniniform ziphodont teeth adapted for stress and strain dissipation. These were adapted to fulfill a completely different role. The incisiform teeth would be effective at grabbing and holding prey items and resisting prey struggle forces compared to the caniniform teeth which could buffer greater stress before transmitting to the surrounding jaw. The teeth of *Dimetrodon* effectively acted as a multi-purpose tool for any situation. The post-caniniform teeth were not adapted for breaking bone. These teeth performed the worst of all those evaluated, experiencing a break from the applied

force of 4000N. In a full bite scenario, contact between the other two tooth types would already occur before these cheek teeth interacted with a food item, lessening the experienced load. In mammalian dentitions, the cheek teeth are often used for grinding and maceration, and this would be the only instance when these teeth are exclusively loaded. If *Dimetrodon* bit down with its full bite force on these teeth they would shatter, indicating they were not used separately from the other teeth during oral processing. This indicates that *Dimetrodon* was unlikely to comminute bone during scavenging, explaining the limited tooth marks on bones from these Permian ecosystems (Schulte et al., 2021).

The upper jaw appears adapted to dissipate stress from the teeth surrounding the raised diastema in *Dimetrodon*. Prevalent among many therapsids and later mammals, the diastema is often closely associated with heterodonty (Huttenlocker et al., 2021). In *Dimetrodon,* this gap may have been used as a 'trap' for small prey to be captured in during predation (Romer and Price, 1940). The length of the mandible is such that the largest and anterior-most teeth close at this gap between the pre-maxilla and maxillary bones. This could effectively hold small prey between the premaxillary and maxillary teeth, allowing for a clean puncturing blow from the lower caniniform teeth. This direct interaction between the mandible and the diastema is unique when compared to other sphenacodontians (Spindler 2020.) Large caniniform teeth with ziphodont morphologies may be best adapted for slicing large sections of flesh and function optimally with increased size relative to the rest of the jaw. A continuous tooth row would aid in capturing and holding of smaller prey but decrease the force exerted by a single serrated tooth by increasing the area of contact. The increased biomechanical accommodation

for the upper caniniform teeth while maintaining premaxillary articulation of the mandible may have been the trigger for the development of the premaxillary step to accommodate both features into the dentition.

Conclusions

MDA varied from the dry skull method of estimating bite force. The most reptilian model was evaluated to be the strongest at 4000N mm^2 despite being predicted by the dry skull method to be the weakest. The more mammalian-style models performed much better in the dry skull estimation method with larger temporalis and masseter muscles. Muscle systems with less specialized adductor muscle force distributions may be under-predicted by mathematical standard models and should be approached with caution. Finite Element Analysis showed that the more specialized dental morphologies in *Dimetrodon*'s jaw could dissipate 4000N of force through the jaw in addition to a vector added to represent prey struggle. The post-caniniform teeth were less able to resist these forces and would break under this pressure. The high bite force and efficiency of muscle translation supports a role of hypercarnivory in *Dimetrodon*, as it would have been able to produce and bear forces required to hunt large-bodied herbivores. The serrated caniniform teeth were best suited for high stress and strain energies. *Dimetrodon* may have scavenged a free meal but was unlikely to be breaking apart bone for marrow as seen in other scavengers.

References

Barghusen, H.R., 1973. The Adductor Jaw Musculature of *Dimetrodon* (Reptilia, Pelycosauria). Journal of Paleontology 47, 823–834.

Bates, K.T., Wang, L., Dempsey, M., Broyde, S., Fagan, M.J., Cox, P.G., 2021. Back to the bones: do muscle area assessment techniques predict functional evolution across a macroevolutionary radiation? Journal of the Royal Society Interface 18, 8.

Bright, J.A., 2014. A Review of Paleontological Finite Element Models and Their Validity. Journal of Paleontology 88, 760–769.

Brink, K.S., Reisz, R.R., 2012. Morphology of the palate and braincase of *Dimetrodon milleri*. Historical Biology 24, 453–459.

Brink, K.S., Reisz, R.R., 2014. Hidden dental diversity in the oldest terrestrial apex predator *Dimetrodon*. Nature Communications 5.

Brocklehurst, N., Brink, K.S., 2017. Selection towards larger body size in both herbivorous and carnivorous synapsids during the Carboniferous. FACETS 2, 68–84.

Brocklehurst, N., Day, M.O., Rubidge, B.S., Fröbisch, J., 2017. Olson's Extinction and the latitudinal biodiversity gradient of tetrapods in the Permian. Proceedings of the Royal Society B: Biological Sciences 284.

Brocklehurst, N., Dunne, E.M., Cashmore, D.D., Fröbisch, J., 2018. Physical and environmental drivers of Paleozoic tetrapod dispersal across Pangaea. Nature Communications 9.

Broyde, S., Dempsey, M., Wang, L., Cox, P.G., Fagan, M., Bates, K.T., 2021. Evolutionary biomechanics: hard tissues and soft evidence? Proc. R. Soc. B. 288, rspb.2020.2809, 20202809.

Buchanan, T.S., 1995. Evidence that maximum muscle stress is not a constant: differences in specific tension in elbow flexors and extensors. Medical Engineering & Physics 17, 529–536.

Crompton, A.W., Parkyn, D.G., 1963. On the Lower Jaw of *Diarthrognathus* and the Origin of the Mammalian Lower Jaw. Proceedings of the Zoological Society of London 140, 697–749.

DeMar, R., Barghusen, H.R., 1972. Mechanis and the Evolution of the Synapsid Jaw. Evolution 26, 622.

Dilkes, D.W., Hutchinson, J.R., Holliday, C.M., Witmer, L.M., Brett-Surman, M.K., Holtz, T.R., Farlow, J.O., 2012. Reconstructing the musculature of dinosaurs, in: The Complete Dinosaur. Indiana University Press, pp. 151–191.

Fox, R.C., 1964. The Adductor Muscles of the Jaw in Some Primitive Reptiles. University of Kansas.

Huttenlocker, A.K., Singh, S.A., Henrici, A.C., Sumida, S.S., 2021. A Carboniferous synapsid with caniniform teeth and a reappraisal of mandibular size-shape heterodonty in the origin of mammals. R. Soc. open sci. 8, 211237.

Jones, M.E.H., Curtis, N., O'Higgins, P., Fagan, M., Evans, S.E., 2009. The head and neck muscles associated with feeding in *Sphenodon* (Reptilia: Lepidosauria: Rhynchocephalia). Paleontologica Electronica 12, 56.

Lautenschlager, S., 2015. Estimating cranial musculoskeletal constraints in theropod dinosaurs. R. Soc. open sci. 2, 150495.

Law, C.J., Mehta, R.S., 2019. Dry versus wet and gross: Comparisons between the dry skull method and gross dissection in estimations of jaw muscle cross-sectional area and bite forces in sea otters. Journal of Morphology 280, 1706–1713.

Moazen, M., Curtis, N., Evans, S.E., O'Higgins, P., Fagan, M.J., 2008. Combined finite element and multi-body dynamics analysis of biting in a *Uromastyx hardwickii* lizard skull. Journal of Anatomy 213, 499–508.

Olson, E.C., 1966. Community Evolution and the Origin of Mammals. Ecology 47, 291–302.

Parrington, F.R., 1955. On the cranial anatomy of some gorgonopsids and the synapsid middle ear. Proceedings of the Zoological Society of London 125, 1–40.

Pearson, M.R., Benson, R.B.J., Upchurch, P., Fröbisch, J., Kammerer, C.F., 2013. Reconstructing the diversity of early terrestrial herbivorous tetrapods. Palaeogeography, Palaeoclimatology, Palaeoecology 372, 42–49.

Reisz, R.R., 1987. Pelycosauria: Handbuch Der Palaoherpetologie. Lubrecht & Cramer.

Romer, A.S., Price, L.W., 1940. Review of the Pelycosauria. Geological Society of America.

Sakamoto, M., 2021. Assessing bite force estimates in extinct mammals and archosaurs using phylogenetic predictions. Palaeontology 64, 743–753.

Spindler, F., 2020. A faunivorous early sphenacodontian synapsid with a diastema. Palaeontologia Electronica 23.

Schulte, C., Flis, C.J., Simon, H., Vollmer, E., 2021. Tooth mark analysis of Dimetrodon appendicular skeletal elements with implications of feeding strategies.

Thomason, J.J., 1991. Cranial strength in relation to estimated biting forces in some mammals. Canadian Journal of Zoology 69, 2326–2333.

Watson, D.M.S., 1948. *Dicynodon* and its allies. Proceedings of the Zoological Society of London 118, 823.

Weijs, W., Hillen, B., 1985. Cross-sectional areas and estimated intrinsic strength of the human jaw muscles. Acta Morphologica Neerlando-Scandinavica 23, 267–274.

Whitney, M.R., LeBlanc, A.R.H., Reynolds, A.R., Brink, K.S., 2020. Convergent dental adaptations in the serrations of hypercarnivorous synapsids and dinosaurs. Biol. Lett. 16, 20200750.

Supplementary Tables

Muscle Topology	Muscle Name	Measured Volume (cm^3)	Measured Fibre Length (cm)	Cross Sectional Area (cm^2)	FMus (N)	Lever Arm (cm)	Dry Skull (N)
Para-reptile	MAME	51.1	9.94	5.13	1540	8.76	1250
	MAMIPs	23.9	9.59	2.49	747	14.4	
	Post. MAMIPt	26.6	7.81	3.40	1020		
	Ant. MAMIPt	22.0	5.71	3.86	1160		
	MAP	7.65	10.1	0.76	228		
Rhynchocephalian	Masseter	23.9	5.40	4.43	1330	11.1	2470
	Temporal	151	14.9	10.1	3040	10.9	
	Post. Pterygoid	32.7	5.40	6.05	1820		
	Ant. Pterygoid	7.13	11.3	0.63	189		
Proto mammalian	Masseter	34.4	3.88	8.88	2660	11.2	1820
	Temporal	54.8	16.2	3.39	1020	5.32	
	Post. Pterygoid	64.3	15.9	4.04	1210		
	Ant. Pterygoid	30.2	14.8	2.04	612		

Table 3:Reconstructed model measurements and calculated force estimates based on the size of the temporalis and masseter or equivalencies.

Supplementary Figures

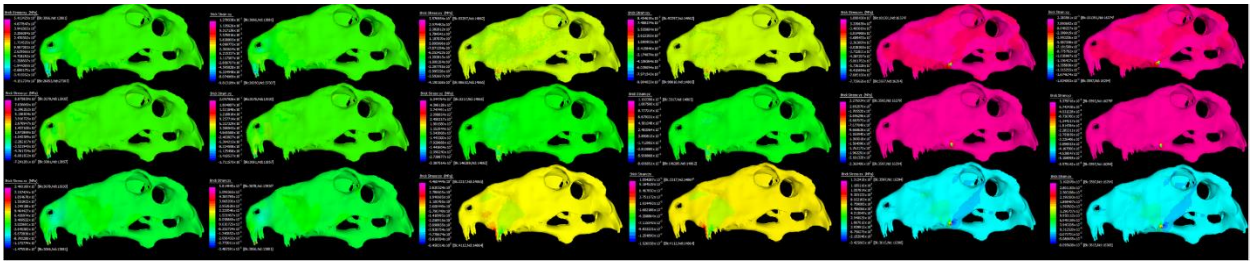

Fig 6 Supplementary Component Stress

From a 4000N force applied along the z-axis to selected heterodont dentition.

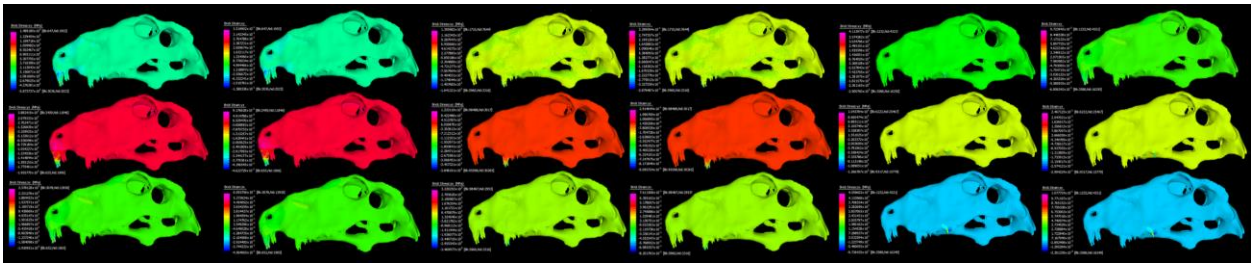

Fig 7 Supplementary Component Stress with Prey Struggle

As a 1000N lateral force in addition to a 4000N force applied along the z-axis to selected heterodont dentition.

Chapter 4: Conclusions

In this thesis I used biomechanical analysis to evaluate the oral processing of *Dimetrodon* as it underwent a series of evolutionary changes to its dental morphology. This was the first use of finite element analysis (FEA) in *Dimetrodon,* and first time the method has been applied for the study of denticles, plicidentine, and the combined performance of enamel, dentine, alveolar bone, and cortical bone material properties. Additionally, I performed an adductor musculature efficiency comparison to verify attachment topology and provide a new maximum to the effective bite force of the animal. This was completed with the first application of multi-body dynamic analysis (MDA) in an early synapsid. Utilising a combination of MDA and FEA methodology, I examined the ecology of an apex predator of a new terrestrial community structure in the Early Permian and addressed a series of hypotheses:

Hypothesis #1: If the caniniform teeth transfer less stress onto the skull than the incisiform teeth, then *Dimetrodon*'s skull is preferentially mitigating kinetic energy surrounding this tooth position. Principles of biomechanical efficacy combined with inferences from extant tetrapods can inform feeding behaviours relating to heterodont dentitions in *Dimetrodon*.

In the heterodont jaws of *Dimetrodon,* the three different tooth morphologies performed at various levels of effectiveness. The serrated caniniform teeth were best suited for high stress and strain energies, followed by the incisiform teeth. The post-

caniniform teeth were unable to support 4000N of force on their own and would break along the crown before the energy was able to reach the root. As these teeth are often used for crushing in mammalian scavengers, *Dimetrodon* would not likely have been breaking apart bone for marrow using the postcanine teeth as seen in other scavengers. Possible oral processing by *Dimetrodon* include scrapes and punctures, but not associated with broken ossified elements.

Hypothesis #2: If the tooth microstructure becomes more biomechanically efficient through evolutionary time, then *Dimetrodon* is adapting for greater masticatory loads, indicating a changing diet.

We found material properties have a significant role in the modelling of the teeth of *Dimetrodon*. The morphology of *Dimetrodon* enamel along the carinae has a notable influence on how energies entered the dentine core of the crown. Smooth enamel transmitted energy homogeneously, creating a single smooth gradient pattern. Serrated enamel was able to contain greater stress energies but transmitted them through the EDJ primarily between denticles. Compared to the smooth enamel, this created numerous, localized gradients associated with the non-uniform denticle pattern. Over time, this would highlight vulnerabilities in the tooth and necessitate increased replacement. Serrations develop not to decrease biomechanical pressure on the jaw, but for other purposes such as slicing and processing thicker-bodied prey. The enamel of derived *Dimetrodon* was more susceptible to damage from high kinetic energies but was able to reap the benefits of serrated tooth enamel processing. These virtues drove natural

selection even without the reinforced globular dentine present in other ziphodonts. This suggests increased consumption of prey with thick layers of soft tissue.

The crests of plicidentine folds in the root concentrated energy. The derived condition of an elongate tooth root shared a similar gross pattern of energy distribution, but when distributed over a greater area resulted in lower stress and strain energies. The elongation of the tooth roots took advantage of the available space in the jaw, allowing for each tooth to bear greater masticatory loads.

Hypothesis #3: If the reptilian muscle reconstruction more efficiently transmits force to the teeth on the lower mandible than other proposed reconstructions (rhynchocephalian and mammal), then that topology is supported biomechanically.

Our current hypothesis, the reptilian model, was evaluated to be the strongest at 4000N mm^2 despite being predicted by the dry skull method to be the weakest. Despite the smaller muscles, how they interacted with the jaw elements increased their efficiency over the rhynchocephalian and mammalian styles. The mammalian-style models, with enlarged masseter and temporalis muscles, were predicted to perform much better than the other two by the dry skull method. Muscle systems with greater adductor muscle force distributions may be under-predicted by mathematical standard models and should be approached with caution.

Hypothesis #4: If *Dimetrodon* had a bite force comparable to extant hypercarnivores, then it could effectively consume thick-tissue, large-bodied prey such as *Edaphosaurus*.

A bite force of 4000N falls in similar categories as contemporary *Panthera* (4450N), but not as large as crocodilians (~13 000N) (Erickson et al., 2006, Sakamoto et al., 2010). We, therefore, believe that *Dimetrodon* was fully capable of actively hunting prey larger than itself, and was not limited to eating prey that could fit in its gape.

From this investigation we conclude that *Dimetrodon* was a capable and deadly apex predator. Their muscle topology would have provided them the opportunity to exert high bite forces on anything caught in their jaws. Their largest teeth would have been able to withstand such forces, and with serrated enamel, slice through large sections of flesh with ease. Within the genus transitions were made to the tooth structure to withstand greater forces, which would not be necessary to hunt smaller prey. Biomechanically, *Dimetrodon* would have been able to process the newly emerging large-bodied herbivores and would not have a limited diet restricted by its cranial anatomy.

Literature Cited:

Abler, W.L., 1992. The Serrated Teeth of Tyrannosaurid Dinosaurs, and Biting Structures in Other Animals. Paleobiology 18, 161–183.

Bakker, R.T., 1982. Juvenile-Adult Habitat Shift in Permian Fossil Reptiles and Amphibians. Science 217, 53–55. https://doi.org/10.1126/science.217.4554.53

Bakker, R.T., Flis, C.J., George, C.D., Cook, L.A., Bell, T.H., Zoehfeld, K.W., 2015. *Dimetrodon* and the earliest apex predators: The Craddock bone bed and George Ranch facies show that aquatic prey, not herbivores were key food sources.

Barghusen, H.R., 1973. The Adductor Jaw Musculature of *Dimetrodon* (Reptilia, Pelycosauria). Journal of Paleontology 47, 823–834.

Berman, D.S., Henrici, A.C., Sumida, S.S., Martens, T., 2004. New Materials of *Dimetrodon teutonis (*Synapsida: Sphenacodontidae) From The Lower Permian of Germany. Annals of Carnegie Museum 73, 48–56.

Berman, D.S., Reisz, R.R., Martens, T., Henrici, A.C., 2001. A new species of *Dimetrodon* (Synapsida: Sphenacodontidae) from the Lower Permian of Germany records first occurrence of genus outside of North America. Canadian Journal of Earth Sciences 38, 803–812. https://doi.org/10.1139/cjes-38-5-803

Beschta, R.L., Ripple, W.J., 2009. Large predators and trophic cascades in terrestrial ecosystems of the western United States. Biological Conservation 142, 2401–2414. https://doi.org/10.1016/j.biocon.2009.06.015

Bourgoyne, A.T., Millheim, K.K., Chenevert, M.E. and Young, F.S., 1986. Applied drilling engineering (Vol. 2, p. 514). Richardson: Society of Petroleum Engineers.

Bright, J.A., 2014. A Review of Paleontological Finite Element Models and Their Validity. Journal of Paleontology 88, 760–769.

Brink, K.S., LeBlanc, A.R.H., Reisz, R.R., 2014. First record of plicidentine in Synapsida and patterns of tooth root shape change in Early Permian sphenacodontians. Naturwissenschaften 101, 883–892. https://doi.org/10.1007/s00114-014-1228-5

Brink, K.S., Maddin, H.C., Evans, D.C., Reisz, R.R., 2015. Re-evaluation of the historic Canadian fossil *Bathygnathus borealis* from the Early Permian of Prince Edward Island. Canadian Journal of Earth Sciences 52, 1109–1120. https://doi.org/10.1139/cjes-2015-0100

Brink, K.S., Reisz, R.R., 2014. Hidden dental diversity in the oldest terrestrial apex predator *Dimetrodon*. Nature Communications 5. https://doi.org/10.1038/ncomms4269

Brocklehurst, N., Brink, K.S., 2017. Selection towards larger body size in both herbivorous and carnivorous synapsids during the Carboniferous. FACETS 2, 68–84. https://doi.org/10.1139/facets-2016-0046

Brocklehurst, N., Kammerer, C.F., Fröbisch, J., 2013. The early evolution of synapsids, and the influence of sampling on their fossil record. Paleobiology 39, 470–490. https://doi.org/10.1666/12049

Case, E.C., 1907. Revision of the Pelycosauria of North America. Carnegie Institution of Washington, Washington.

DeMar, R., Barghusen, H.R., 1972. Mechanis and the Evolution of the Synapsid Jaw. Evolution 26, 622. https://doi.org/10.2307/2407058

Dutel, H., Gröning, F., Sharp, A.C., Watson, P.J., Herrel, A., Ross, C.F., Jones, M.E.H., Evans, S.E., Fagan, M.J., 2021. Comparative cranial biomechanics in two lizard species: impact of variation in cranial design. J Exp Biol jeb.234831. https://doi.org/10.1242/jeb.234831

Edelsbrunner, H., Mucke, E.P., 1994. Three-Dimensional Alpha Shapes. ACM Transactions on Graphics 13, 30. https://doi.org/10.1145/174462

Ehrlich, P.J., Lanyon, L.E., 2002. Mechanical Strain and Bone Cell Function: A Review. Osteoporosis International 13, 688–700.

Erickson, G.M., Olson, K.H., 1996. Bite marks attributable to *Tyrannosaurus rex*: Preliminary description and implications. Journal of Vertebrate Paleontology 16, 175–178. https://doi.org/10.1080/02724634.1996.10011297

Fox, R.C., 1964. The Adductor Muscles of the Jaw In Some Primitive Reptiles. University of Kansas.

Huttenlocker, A.K., Rega, E., Sumida, S.S., 2010. Comparative anatomy and osteohistology of hyperelongate neural spines in the sphenacodontids *Sphenacodon* and *Dimetrodon* (Amniota: Synapsida). Journal of Morphology 271, 1407–1421. https://doi.org/10.1002/jmor.10876

Huttenlocker, A.K., Singh, S.A., Henrici, A.C., Sumida, S.S., 2021. A Carboniferous synapsid with caniniform teeth and a reappraisal of mandibular size-shape heterodonty in the origin of mammals. R. Soc. open sci. 8, 211237. https://doi.org/10.1098/rsos.211237

Mann, A., Reisz, R.R., 2020. Antiquity of "Sail-Backed" Neural Spine Hyper-Elongation in Mammal Forerunners. Front. Earth Sci. 8. https://doi.org/10.3389/feart.2020.00083

Moreno, K., Wroe, S., Clausen, P., McHenry, C., D'Amore, D.C., Rayfield, E.J., Cunningham, E., 2008. Cranial performance in the Komodo dragon (Varanus komodoensis) as revealed by high-resolution 3-D finite element analysis. Journal of Anatomy 212, 736–746. https://doi.org/10.1111/j.1469-7580.2008.00899.x

Olson, E.C., 1966. Community Evolution and the Origin of Mammals. Ecology 47, 291–302. https://doi.org/10.2307/1933776

Olson, E.C., 1962. Late Permian Terrestrial Vertebrates, U. S. A. and U. S. S. R. Transactions of the American Philosophical Society 52, 1. https://doi.org/10.2307/1005904

Parrish, W.C., 1978. Paleoenvironmental analysis of a Lower Permian bonebed and adjacent sediments, Wichita County, Texas. Palaeogeography, Palaeoclimatology, Palaeoecology 24, 209–237. https://doi.org/10.1016/0031-0182(78)90043-3

Preuschoft, H., Witzel, U., 2002. Biomechanical investigations on the skulls of reptiles and mammals. Senckenbergiana lethaea 82, 207–222. https://doi.org/10.1007/BF03043785

Reisz, R.R., Berman, D.S., Scott, D., 1992. The cranial anatomy and relationships of *Secodontosaurus*, an unusual mammal-like reptile (Synapsida: Sphenacodontidae) from the early Permian of Texas. Zoological Journal of the Linnean Society 104, 127–184.

Romer, A.S., 1936. Studies On American Permo-Carboniferous Tetrapods.

Romer, A.S., Price, L.W., 1940. Review of the Pelycosauria. Geological Society of America.

Ross, C.F., Metzger, K.A., 2004. Bone strain gradients and optimization in vertebrate skulls. Annals of Anatomy - Anatomischer Anzeiger 186, 387–396. https://doi.org/10.1016/S0940-9602(04)80070-0

Rudwick, M.J.S., 1964. The inference of function from structure in fossils. The British Journal for the Philosophy of Science 15, 27–40. https://doi.org/10.1093/bjps/XV.57.27

Sahney, S., Benton, M.J., Ferry, P.A., 2010. Links between global taxonomic diversity, ecological diversity and the expansion of vertebrates on land. Biology Letters 6, 544–574. https://doi.org/10.1098/rsbl.2009.1024

Sander, P.M., 1989. Early permian depositional environments and pond bonebeds in central Archer County, Texas. Palaeogeography, Palaeoclimatology, Palaeoecology 69, 1–21. https://doi.org/10.1016/0031-0182(89)90153-3

Sellers, W.I., Crompton, R.H., 2004. Using sensitivity analysis to validate the predictions of a biomechanical model of bite forces. Annals of Anatomy - Anatomischer Anzeiger 186, 89–95. https://doi.org/10.1016/S0940-9602(04)80132-8

Spindler, F., 2019. A faunivorous early sphenacodontian synapsid with a diastema. Palaeontol Electron. https://doi.org/10.26879/1023

Sues, H.-D., Reisz, R.R., 1998. Origins and early evolution of herbivory in tetrapods. Trends in Ecology & Evolution 13, 141–145. https://doi.org/10.1016/S0169-5347(97)01257-3

Thomason, J.J., 1991. Cranial strength in relation to estimated biting forces in some mammals. Canadian Journal of Zoology 69, 2326–2333. https://doi.org/10.1139/z91-327

Watson, D.M.S., 1948. *Dicynodon* and its allies. Proceedings of the Zoological Society of London 118, 823.

Whitney, M.R., LeBlanc, A.R.H., Reynolds, A.R., Brink, K.S., 2020. Convergent dental adaptations in the serrations of hypercarnivorous synapsids and dinosaurs. Biol. Lett. 16, 20200750. https://doi.org/10.1098/rsbl.2020.0750